UNIVERSIDADE FEDERAL DO CEARÁ
CENTRO DE TECNOLOGIA
DEPARTAMENTO DE ENGENHARIA DE TELEINFORMÁTICA
PROGRAMA DE PÓS GRADUAÇÃO EM ENGENHARIA DE TELEINFORMÁTICA

PEDRO MARINHO RAMOS DE OLIVEIRA

PARATUCK-N SEMI-BLIND RECEIVERS FOR MULTI-HOP COOPERATIVE MIMO RELAY SYSTEMS

FORTALEZA
2017

PEDRO MARINHO RAMOS DE OLIVEIRA

PARATUCK-N SEMI-BLIND RECEIVERS FOR MULTI-HOP COOPERATIVE MIMO RELAY SYSTEMS

Dissertação apresentada ao Programa de Pós-Graduação em Engenharia de Teleinformática da Universidade Federal do Ceará, como requisito parcial à obtenção do título de Mestre em Engenharia de Teleinformática. Área de concentração: Sinais e Sistemas.

Orientador: Prof. Dr. Carlos Alexandre Rolim Fernandes.

FORTALEZA
2017

Dados Internacionais de Catalogação na Publicação
Universidade Federal do Ceará
Biblioteca Universitária
Gerada automaticamente pelo módulo Catalog, mediante os dados fornecidos pelo(a) autor(a)

O49p Oliveira, Pedro Marinho Ramos de.
PARATUCK-N Semi-Blind Receivers for Multi-Hop Cooperative MIMO Relay Systems / Pedro Marinho Ramos de Oliveira. – 2017.
63 f. : il. color.

Dissertação (mestrado) – Universidade Federal do Ceará, Centro de Tecnologia, Programa de Pós-Graduação em Engenharia de Teleinformática, Fortaleza, 2017.
Orientação: Prof. Dr. Carlos Alexandre Rolim Fernandes.

1. Sistemas Cooperativos. 2. MIMO. 3. PARATUCK-N. 4. Receptores Semi-Cegos. 5. Produto de Kronecker. I. Título.

CDD 621.38

PEDRO MARINHO RAMOS DE OLIVEIRA

PARATUCK-N SEMI-BLIND RECEIVERS FOR MULTI-HOP COOPERATIVE MIMO RELAY SYSTEMS

Dissertation presented to the Coordination of the Teleinformatics Engineering Post-Graduation Program of the Universidade Federal do Ceará as a part of the requisites to obtain the Master's Degree in Teleinformatics Engineering. Concentration Area: Signals and Systems.

Approved in 28/07/2017.

COMMITTEE

Prof. Dr. Carlos Alexandre Rolim Fernandes (Orientador)
Universidade Federal do Ceará (UFC)

Prof. Dr. André Lima Ferrer de Almeida
Universidade Federal do Ceará (UFC)

Prof. Dr. Leandro Rochini Ximenes
Universidade Estadual de Campinas (UNICAMP)

I dedicate this work to God, my family, friends, and all the people who helped me during my Master's degree period.

ACKNOWLEDGMENTS

In the first place, I thank God to give me conditions to study and conclude the Master's degree in Teleinformatics Engineering in one of the best post graduation programs in Brazil.

I thank my Family, specially my parents, Nertan Oliveira and Hylana Oliveira, who always support me in anything I do and were presents in this important period of my life.

I also thank my supervisor, Carlos Alexandre, for the great help in the developed of this work and all the works that we made during the Master's period, as well as for the compromising and for the great contribution in my academic career, and all the professors that I met during the classes for the knowledge that was given me.

At last, but not less important, I thank all my friends that helped me during my Master's period, sharing with me experiences, knowledge, good and bad moments.

RESUMO

Sistemas de comunicações cooperativas são um importante campo de pesquisa atualmente devido às vantagens que oferecem, como o aumento da potência recebida, melhor qualidade de sinal e ganhos de diversidade espacial. Particularmente, sitemas *multi-hop* (quando vários *relays* são usados em série) são uma importante parte das comunicações cooperativas, uma vez que tais sistemas precisam de menos potência de transmissão se comparados a sistemas *two-hop* (quano apenas um único *relay* é usado). Por outro lado, sistemas MIMO (*Multiple-Input Multiple-Output*) estão presentes em diversos padrões de comunicação, provendo algumas vantagens, como ganhos de multiplexação e diversidade espacial. Com base nesse cenário, o presente trabalho propõe dois receptores semi-cegos baseados no produto de Kronecker que estimam conjuntamente os símbolos e os canais de um sistema AF (*Amplify-and-Forward*) MIMO cooperativo com multiplos saltos. O protocolo AF é bastante usado em redes cooperativas devido à sua grande performance e fácil implementação, que consiste basicamente em amplificar e retransmitir o sinal recebido pelo *relay*. É considerado um esquema de transmissão usando uma codificação simplificada KRST (*Khatri-Rao Space-Time*) na fonte, combinada com um esquema AF nos *relays*. É mostrado que o tensor de terceira ordem dos sinais recebidos pelo destino satisfazem uma decomposição tensorial PARATUCK-(K+1), em que K é o número de *relays*. Esse modelo tensorial permite uma estimação semi-cega dos símbolos e canais, com o uso de alguns símbolos pilotos. O primeiro algoritmo, chamado de Least-Squares Kronecker Factorization (LS-KF), é baseado em uma fatorização da matrix do produto de Kronecker entre as matrizes de símbolos e de canal. Já o outro algoritmo, chamado de Least-Squares Kronecker Rearrangement-Based (LS-KR), é baseado no rearranjo dessa matrix do produto de Kronecker, com o objetivo de conseguir uma matrix com rank 1. A performance desses receptores é avaliada através do resultado de simulações computacionais, provando sua eficiência em estimar os canais e prover uma baixa SER (*Symbol Error Rate*). Os algoritmos propostos no cenário *multi-hop* são comparados um com o outro, com os cenários *two-hop* e *three-hop*, e com outros dois algoritmos (PARATUCK2-ZF and PARATUCK2-ALS). Os algoritmos propostos no cenário *multi-hop* tiveram melhor performance em todas as simulações, se comparado com o cenário *two-hop*, resultando numa menor SER e melhores estimações dos canais.

Palavras-Chave: Sistemas Cooperativos. MIMO. PARATUCK-(K+1). Produto de Kronecker. Receptores Semi-Cegos. Multi-Saltos. AF.

ABSTRACT

Cooperative communication systems are a promising research field nowadays due to its advantages, like the increase of the received power, better quality of signal and spatial diversity gains. Specifically, multi-hop systems (when several relays are used in a serial way) are a very important part of cooperative communications, since they have the advantage of needing less transmission power than the two-hop systems (when a single relay is used). Also, Multiple-Input Multiple-Output (MIMO) systems are present in several standards of communications, providing some advantages, like the spatial and multiplexing gains. Based on this scenario, this work proposes two semi-blind receivers based on the Kronecker product that jointly estimate the symbol and the channels in a multi-hop Amplify-and-Forward (AF) MIMO relay-assisted system. The AF protocol is widely used in cooperative networks due to its great performance and easy implementation, consisting in basically amplifying and re-transmitting the received signal by the relay. We consider a transmission scheme using a simplified Khatri-Rao Space-Time (KRST) coding at the source node, combined with an AF scheme at the relay nodes. We show that the third-order tensor of signals received by the destination node satisfies a PARATUCK-(K+1) decomposition, where K is the number of relays. This tensorial modeling enables a semi-blind estimation of symbols and channels with the use of a few pilot symbols. The first receiver, called Least-Squares Kronecker Factorization (LS-KF), is based on a factorization of the Kronecker product between the symbol matrix and a channel matrix. The other receiver, called Least-Squares Kronecker Rearrangement-Based (LS-KR), is based on a rearrangement of this Kronecker product matrix, in order to achieve rank-1 matrices. The performance of these receivers is evaluated by means of computational simulation results, proving their efficiency in estimating the channels and, hence, providing a low Symbol Error Rate (SER). The proposed algorithms in the multi-hop scenario were compared to each other, with the two-hop and three-hop scenarios, and with two other algorithms (PARATUCK2-ZF and PARATUCK2-ALS). The proposed algorithms in the multi-hop scenario were better at all simulations, if comparing to the two-hop scenario, providing a lower SER and better channels estimations.

Keywords: Cooperative Systems. MIMO. PARATUCK-(K+1). Kronecker Product. Semi-Blind Receivers. Multi-Hop. AF.

LIST OF FIGURES

LIST OF TABLES

ACRONYMS

AF	Amplify-and-Forward
DF	Decode-and-Forward
CF	Compress-and-Forward
SISO	Single-Input Single-Output
MISO	Multiple-Input Single-Output
SIMO	Single-Input Multiple-Output
MIMO	Multiple-Input Multiple-Output
KRST	Khatri-Rao Space-Time
SVD	Singular-Value Decomposition
PARAFAC	Parallel Factor Analysis
CANDECOMP	Canonical Decomposition
CP	Candecomp-Parafac
NTD	Nested Tucker Decomposition
TDMA	Time Division Multiple Access
FDMA	Frequency Division Multiple Access
CSI	Channel State Information
CSIT	Channel Side Information at the Transmitter
CSIR	Channel Side Information at the Receiver
ALS	Alternating Least Squares
TST	Tensor Space-Time
OFDM	Orthogonal Frequency Division Multiplexing
CDMA	Code Division Multiple Access
STF	Space-Time Frequency
LS	Least Squares
LS-KF	Least-Squares Kronecker Factorization
LS-KR	Least-Squares Kronecker Rearrangement-Based
KR	Kronecker Rearrangement
QAM	Quadrature Amplitude Modulation
PSK	Phase Shift Keying
SNR	Signal-to-Noise Ratio
AWGN	Additive White Gaussian Noise
ZF	Zero-Forcing
SER	Symbol Error Rate
NMSE	Normalized Minimum Square Error

NOTATION

Scalars, vectors, matrices, and tensors are represented, respectively, by lower-case (a, b, c, ...), boldface lower-case (**a**, **b**, **c**, ...), boldface capital (**A**, **B**, **C**, ...), and calligraphic ($\mathcal{A}$, $\mathcal{B}$, $\mathcal{C}$, ...) letters. If nothing else is explicitly stated, the meaning of the following symbols are:

a^*	complex conjugate of $a \in \mathbb{C}$
$\|\mathbf{a}\|$	absolute value of **a**
$\|\|\mathbf{A}\|\|_F$	Frobenius norm of **A**
$\mathbf{A}^T$	transpose of **A**
$\mathbf{A}^H$	Hermitian transpose of **A**
$\mathbf{A}^{-1}$	inverse of **A**
$\mathbf{A}^\dagger$	Moore-Penrose pseudo-inverse of **A**
$\mathbf{a}_i = a_i$	$(i)^{th}$-element of vector $\mathbf{a} \in \mathbb{C}^I$
$\mathbf{A}_{i_1,i_2} = a_{i_1,i_2}$	$(i_1, i_2)^{th}$-element of matrix $\mathbf{A} \in \mathbb{C}^{I_1 \times I_2}$
$\mathbf{A}_{i_1.}$	${i_1}^{th}$ row of **A**
$\mathbf{A}_{.i_2}$	${i_2}^{th}$ column of **A**
$\mathbf{A}_{i_1,i_2,i_3} = a_{i_1,i_2,i_3}$	$(i_1, i_2, i_3)^{th}$-element of tensor $\mathcal{A} \in \mathbb{C}^{I_1 \times I_2 \times I_3}$
$\mathbf{A}_{i_1..} \in \mathbb{C}^{I_2 \times I_3}$	${i_1}^{th}$ first-mode matrix-slice of tensor $\mathcal{A}$
$\mathbf{A}_{.i_2.} \in \mathbb{C}^{I_3 \times I_1}$	${i_2}^{th}$ first-mode matrix-slice of tensor $\mathcal{A}$
$\mathbf{A}_{..i_3} \in \mathbb{C}^{I_1 \times I_2}$	${i_3}^{th}$ first-mode matrix-slice of tensor $\mathcal{A}$
$\mathbf{a} \circ \mathbf{b}$	outer product between **a** and **b**
$\mathbf{A} \otimes \mathbf{B}$	Kronecker product of **A** with **B**
$\mathbf{A} \diamond \mathbf{B}$	Katri-Rao product between **A** and **B**
$vec(\mathbf{A})$	vectorization of matrix **A**
$unvec(\mathbf{a})$	unvectorization of vector **a** to its former matrix
$diag(\mathbf{a})$	diagonal matrix with diagonal entries given by the elements of **a**
$D_p(\mathbf{A})$	diagonal matrix with diagonal entries given by the elements of the p^{th} row of **A**
$SVD(\mathbf{A})$	singular-value decomposition of **A**
$\boldsymbol{I}_N$	a $N \times N$ identity matrix
$\mathbf{1}_{M \times N}$	a $M \times N$ matrix full of ones

SUMMARY

Chapter 1

INTRODUCTION

1.1 Context and Motivation

Aiming to provide a considerable increase in the received power and a better signal quality, the concept of cooperative communications relay systems was developed, in which at least one relay node is used to assist the communication between the source node and the destination node [1]. Another advantage provided by cooperative communications is the spatial diversity gain due to the allocation of the relays. A cooperative communication can be done according to several protocols, that are classified in fixed (Amplify-and-Forward (AF), Decode-and-Forward (DF), Compress-and-Forward (CF), and others) and adaptive (selective decode-and-forward, incremental relaying, and others). In fixed protocols, the resources of the system are divided in a fixed way between the source and relays, while in the adaptive schemes these resources are not divided in deterministic way. In this work, the fixed AF protocol is used, due to its easy implementation and great performance.

Moreover, multi-hop systems, i.e, cooperative systems with several relays connected in a serial way, have the advantage of needing less transmission power than two-hop networks (only one relay), as the distance between the source and the destination is divided in several smaller links.

Furthermore, Multiple-Input Multiple-Output (MIMO) systems provide a great advance in the wireless communication field, due to its considerable increase in the coverage area, capacity and spatial diversity gain. This technology quickly developed and is widely used nowadays, being present in several standards (WIMAX-IEEE 802.16, WLAN-IEEE 802.11N, and many others) [2]. In cooperative MIMO, a particular area of MIMO systems, all the nodes have multiple antennas, increasing the spatial multiplexing gains. This particular scenario provides a distributed spatial diversity gain, due to the relays, and a concentrated spatial diversity gain, due to the multiple antennas in all nodes.

On the other hand, due to its advantages in exploring the multidimensional nature of the signals, tensor decompositions are applied in several areas, including digital signal processing [3], [4], [5]

and telecommunications [6], [7], [8]. Also, tensor analysis has shown to be an efficient approach for channel and/or symbol estimation in cooperative MIMO systems [9], [10], [11], [12], [13]. A very important field of research in tensor algebra is the study of tensor decompositions, which are a very useful tool regarding the analysis of multilinear problems. Tensor decompositions have some advantages like their uniqueness properties and the fact that the rank can exceed the tensor dimensions. Examples of tensor decompositions are the PARAllel FACtor/CANonical DECOMPosition (PARAFAC/CANDECOMP) [26] [27], Tucker [25], PARATUCK [15], etc.

Due to its simplicity, as previously explained, in this work it is considered an AF relaying system. More specifically, it is considered a multi-hop scenario, with a multiple-antenna source node, K multiple-antenna AF relay nodes and a multiple-antenna destination node. This scenario is an one-way half-duplex relaying system, where the source node transmits to the destination during $K + 1$ consecutive transmission phases.

In this work, we propose two semi-blind non-iterative receivers based on the Kronecker product. These receivers jointly estimate the symbol and the channels in a multi-hop AF MIMO cooperative system. It is used a simplified Khatri-Rao Space-Time (KRST) coding [14] at the source node, combined with an AF coding scheme at the relay nodes. The third-order tensor of signals received by the destination node satisfies a PARATUCK-(K+1) decomposition [15], where K is the number of relays, enabling a semi-blind estimation of symbols and channels using of a few pilot symbols. We propose two non-iterative receivers algorithms that are based on the Kronecker product. In the first one, Singular-Value Decomposition (SVD) is used to jointly estimate the symbol, the channel of the last hop link and a global channel that contains information of the other links. The second one is based on a rearrangement of the Kronecker product matrix between the symbols and channel matrices proposed in [16], this rearrangement of the Kronecker product matrix is done in order to achieve a rank-1 matrix. The symbols and the matrix of the last hop are estimated using the SVD of the achieved rank-1 matrix and the so-called global channel is estimated as in the first algorithm. These algorithms have the advantage of being non-iterative, providing a good performance. Also, the multi-hop cooperative systems provide an additional advantage due to its transmission power gain, as previously described.

The performance of these algorithms are evaluated by means of computational simulations using Monte Carlo runs. The metrics used to asses the performance are the Symbol Error Rate (SER) and the Normalized Minimum Square Error (NMSE) of the estimated channel.

1.2 Contributions

The major and original contributions of this work are the development and the performance evaluation of two new non-iterative receivers algorithms that are based on the Kronecker product in a multi-hop AF MIMO cooperative system. More specifically, the present work contributed with:

- System modeling using the PARATUCK-N tensor model.
- Developing of equations that express the received signal in the PARATUCK-N tensor model as a Kronecker product matrix.
- Proposition of a new non-iterative receiver algorithm that is based on the factorization of the Kronecker product matrix.
- Proposition of a new non-iterative receiver algorithm that is based on the rearrangement of the Kronecker product matrix.
- Performance evaluation of the new proposed algorithms by means of computational simulations.

1.3 Scientific Production

Partial results of the present dissertation are presented in the following paper:

P. M. R. Oliveira, C. A. R. Fernandes, "*PARATUCK-3 Semi-Blind Receivers for Three-Hop Cooperative MIMO Relay Systems*", XXXV Simpósio Brasileiro de Telecomunicações (SBrT), São Pedro-SP, September 3^{rd} to 6^{th}, 2017.

Also, a journal paper is being developed with the full results of this dissertation.

1.4 Work Structure

The rest of this work is divided as follows:

- Chapter 2 deals with the basics theoretical concepts necessary to the development and understanding of this work. These concepts involve the tensor algebra, in particular the most important tensor decompositions, the basics of cooperative communications and MIMO systems, specially the cooperative MIMO scenario.

- Chapter 3 presents a bibliography review of important works that use the tensor approaches in the field of wireless communication to solve problems that deals with multilinear data. Also, the system modeling using the PARATUCK-N tensor model and the proposed non-iterative semi-blind receivers are presented.
- In Chapter 4 the computational simulation results based on Monte Carlo samples are presented, showing the performance of the proposed algorithms, in many scenarios. This performance is evaluated using the SER and the NMSE.
- At last, Chapter 5 presents the conclusions of this work, as well as the perspectives of future works.

Chapter 2

THEORETICAL BACKGROUND

This chapter is dedicated to present the theoretical background related to the contributions of this work. It is divided in three sections, the first section deals with the basic concepts of tensors and some important tensor decompositions, as well as its representations in different notations (scalar notation, outer product notation, etc). In the second section, cooperative communications and its most popular protocols are discussed. At last, the third section discuss about the concepts and representations of MIMO systems.

2.1 Introduction to Tensors

In this section, it will be discussed the basics concepts of multilinear algebra, as well as some important definitions to the understanding of this work. Tensor decompositions are also the focus of this section.

2.1.1 *Basic Concepts of Tensor Algebra*

In the literature, one can find different definitions of the word tensor. Indeed, depending on the research field, the definition of tensors can be a little bit different. Our approach is focused on digital signal processing [3] [4] [5], where a tensor is used to generalize the representations of scalars, vectors, and matrices. In the literature, one can find several definitions of tensors that leads to the same concept. [18] defines a tensor as a mathematical entity that has multilinearity properties after a change of the coordinate system. In [17] a tensor is defined as a multidimensional array. In other words, a N^{th}-order (or N-way) tensor is a multilinear array that results of the tensor product of N vector spaces, where each one has its own coordinate system. [19] interprets a N^{th}-order tensor as an array that offers a linear dependency regarding to N vector spaces, where the elements of it can be

accessed by N indexes.

In this work, we going to use the definition that treats a tensor as a multidimensional array [17]. A 0-order tensor is a scalar, a 1^{st}-order tensor is a vector, a 2^{nd}-order tensor is a matrix, a 3^{rd}-order tensor is a box, and so on. N^{th}-order tensors, where $N \geq 3$, are called higher-order tensors. The goal of this section is to provide an overview of higher-order tensors, as well as some of its most known decompositions.

Some definitions are very important to the understanding of this work, as, for example, the outer product. Let $\mathcal{X} \in \mathbb{C}^{I_1 \times I_2 \times \ldots \times I_N}$ be a N^{th}-order tensor and $\mathcal{Y} \in \mathbb{C}^{J_1 \times J_2 \times \ldots \times J_M}$ a M^{th}-order tensor. The outer product between these two tensors is given by

$$\mathcal{Z}_{i_1,i_2,\ldots,i_N,j_1,j_2,\ldots,j_M} = [\mathcal{X} \circ \mathcal{Y}]_{i_1,i_2,\ldots,i_N,j_1,j_2,\ldots,j_M} = x_{i_1,i_2,\ldots,i_N} y_{j_1,j_2,\ldots,j_M}. \tag{2.1}$$

The outer product of $\mathcal{X}$ and $\mathcal{Y}$ is another tensor $\mathcal{Z}$, with order given by the sum of the orders of its two former tensors, that is $N + M$.

Now that we defined the concept of outer product of two tensors, lets define the concept of the rank of a tensor. Let $\mathcal{X} \in \mathbb{C}^{I_1 \times I_2 \times \ldots \times I_N}$ be a N^{th}-order tensor. Its rank, denoted by $R(\mathcal{X})$, is the minimal number of rank-1 tensors that linearly combined corresponds to $\mathcal{X}$ [24]. Particularly, a rank-1 tensor can be written as the outer product of N vectors, that is

$$\mathcal{X} = \mathbf{v}^{(1)} \circ \mathbf{v}^{(2)} \circ \ldots \circ \mathbf{v}^{(N)}, \tag{2.2}$$

where $\mathcal{X}$ is the rank-1 tensor and $\mathbf{v}^n \in \mathbb{C}^{I_n}$, for $n = 1 : N$, are the vectors called the components of $\mathcal{X}$. Another important definition in this work is the Frobenius norm of a tensor, that is interpreted as the energy of the tensor. The Frobenius norm of the arbitrary tensor $\mathcal{X}$, is given by

$$||\mathcal{X}||_F = \left(\sum_{i_1=1}^{I_1} \sum_{i_2=1}^{I_2} \ldots \sum_{i_N=1}^{I_N} |x_{i_1,i_2,\ldots,i_N}|^2 \right)^{\frac{1}{2}}. \tag{2.3}$$

Let us see now the definition of matrix slices. The matrix slices of a tensor are all the two-dimensional sections of a tensor, by fixing all but two indices of it [17]. We can see in Figure 2.1 the three modes slices of an arbitrary 3^{rd}-order tensor. At last, let us describe the concept of unfolded matrices of a tensor. The n^{th}-mode unfolded matrix $\mathbf{X}_n$ of a tensor $\mathcal{X} \in \mathbb{C}^{I_1 \times I_2 \times \ldots \times I_N}$ is defined as a $I_n \times I_1 I_2 \ldots I_{n-1} I_{n+1} I_N$ matrix, obtained by stacking all the matrix slices of the tensor. Indeed, by using the definition of slices previously described, we can say that the unfolded matrix is obtained by stacking all the matrix slices of a given mode of the tensor. The way that these slices are stacked depends on the definition of the unfolded matrix.

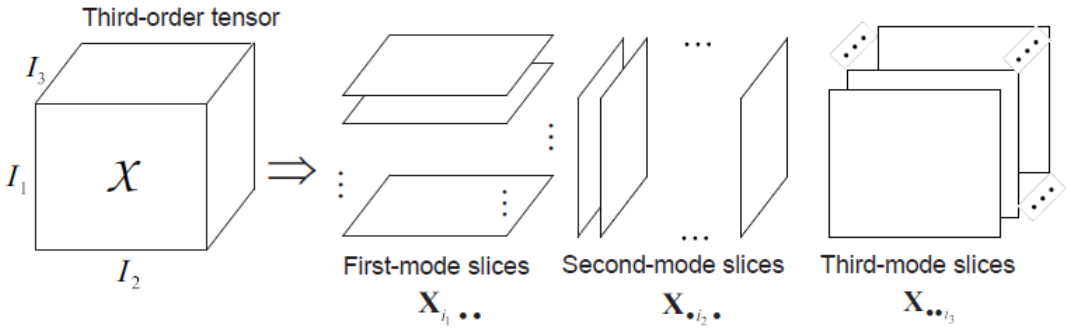

Fig. 2.1: Matrix slices of a 3^{rd}-order tensor. Figure from [24].

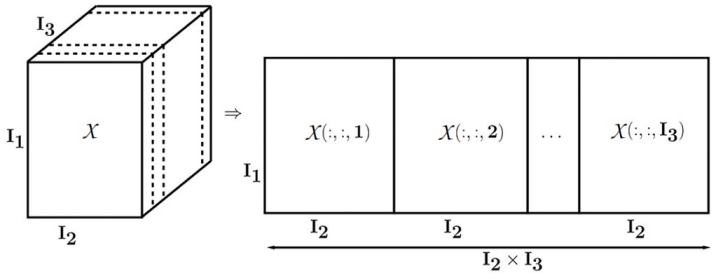

Fig. 2.2: Matrix unfolded of a 3^{rd}-order tensor. Figure from [30].

In Figure 2.2 we can see the mode-1 matrix unfolded $\mathbf{X}_1 \in \mathbb{C}^{I_1 \times I_2 I_3}$ of the arbitrary 3^{rd}-order tensor $\mathcal{X} \in \mathbb{C}^{I_1 \times I_2 \times I_3}$.

2.1.2 *Tensor Decompositions*

In this subsection, some important tensor decompositions are presented. A tensor decomposition is a field of the tensor algebra that represents a tensor as a linear combination of some factors (in the PARAFAC decomposition, the tensor is represented by a linear combination of outer product factors, as we will see in this section). Tensor decompositions are a very useful tool in problems where a multilinear data that contain different contributions must be identified from a measured data [24], as, for example, in the analysis of wireless signals, the case studied in this work.

Parallel Factor (PARAFAC) Decomposition

The PARAFAC decomposition (or CANDECOMP, or even CP (Candecomp-Parafac)) [26] [27], was developed by Harshman and Carol & Chang in different works in 1970. Considering a 3^{rd}-order tensor, we can say that this decomposition is a sum of triple products, or equivalently, a sum of several

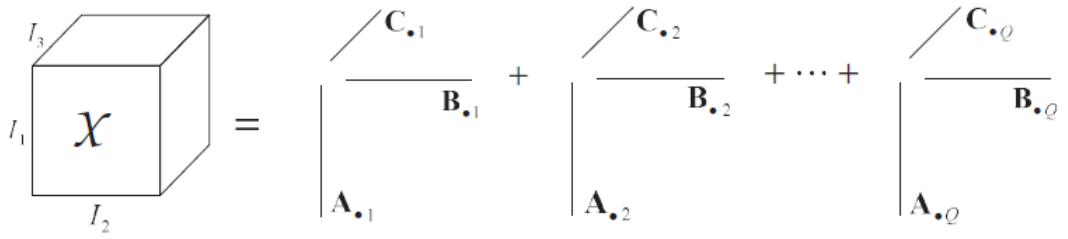

Fig. 2.3: Illustration of the PARAFAC decomposition as a sum of rank-1 tensors. Figure from [24].

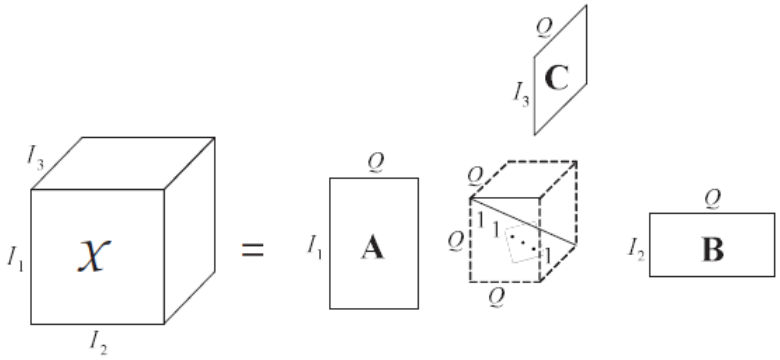

Fig. 2.4: Illustration of the PARAFAC decomposition as a particular case of the Tucker-3 decomposition. Figure from [24].

rank-1 tensors. The PARAFAC decomposition of a 3^{rd}-order tensor $\mathcal{X} \in \mathbb{C}^{I_1 \times I_2 \times I_3}$ can be written in scalar form as

$$x_{i_1,i_2,i_3} = \sum_{q=1}^{Q} a_{i_1,q} b_{i_2,q} c_{i_3,q}, \tag{2.4}$$

where $a_{i_1,q}$, $b_{i_2,q}$ and $c_{i_3,q}$ are the scalar components of the matrices $\mathbf{A}^{I_1 \times Q}$, $\mathbf{B}^{I_2 \times Q}$ and $\mathbf{C}^{I_3 \times Q}$, respectively, and Q is the rank of the decomposition (or the number of factors). The PARAFAC decomposition can also be written using the outer product notation as

$$\mathcal{X} = \sum_{q=1}^{Q} \mathbf{A}_{.q} \circ \mathbf{B}_{.q} \circ \mathbf{C}_{.q}. \tag{2.5}$$

A 3^{rd}-order PARAFAC decomposition is illustrated in Figure 2.3 as a sum of Q rank-1 tensors. The PARAFAC decomposition can be interpreted as a particular case of the Tucker-3 decomposition with an identity core tensor, as shown in Figure 2.4.

We can represent the three slices of the PARAFAC decomposition of the 3^{rd}-order tensor previously defined as

$$\mathbf{X}_{i_1..} = \mathbf{B} D_{i_1}(\mathbf{A}) \mathbf{C}^T. \tag{2.6}$$

$$\mathbf{X}_{.i_2.} = \mathbf{C}D_{i_2}(\mathbf{B})\mathbf{A}^T. \tag{2.7}$$

$$\mathbf{X}_{..i_3} = \mathbf{A}D_{i_3}(\mathbf{C})\mathbf{B}^T. \tag{2.8}$$

If we stack these first-, second- and third-mode slices, we will have the matrices unfolded given by

$$\mathbf{X}_1 = \begin{bmatrix} \mathbf{X}_{..1} \\ \vdots \\ \mathbf{X}_{..I_3} \end{bmatrix} = \begin{bmatrix} \mathbf{A}D_1(\mathbf{C}) \\ \vdots \\ \mathbf{A}D_{I_3}(\mathbf{C}) \end{bmatrix} \mathbf{B}^T = (\mathbf{C} \diamond \mathbf{A})\mathbf{B}^T. \tag{2.9}$$

$$\mathbf{X}_2 = \begin{bmatrix} \mathbf{X}_{1..} \\ \vdots \\ \mathbf{X}_{I_1..} \end{bmatrix} = \begin{bmatrix} \mathbf{B}D_1(\mathbf{A}) \\ \vdots \\ \mathbf{B}D_{I_1}(\mathbf{A}) \end{bmatrix} \mathbf{C}^T = (\mathbf{A} \diamond \mathbf{B})\mathbf{C}^T. \tag{2.10}$$

$$\mathbf{X}_3 = \begin{bmatrix} \mathbf{X}_{.1.} \\ \vdots \\ \mathbf{X}_{.I_2.} \end{bmatrix} = \begin{bmatrix} \mathbf{C}D_1(\mathbf{B}) \\ \vdots \\ \mathbf{C}D_{I_2}(\mathbf{B}) \end{bmatrix} \mathbf{A}^T = (\mathbf{B} \diamond \mathbf{C})\mathbf{A}^T. \tag{2.11}$$

The PARAFAC decomposition can be unique for ranks greater than one up to scaling and permutation factors. To understand the PARAFAC uniqueness condition, lets first define the concept of Kruskal-rank (k-rank), proposed by Kruskal in [31].

The k-rank of a matrix $\mathbf{A} \in \mathbb{C}^{I_1 \times Q}$ is the maximum number k such that every set of k columns of **A** is linearly independent. We can see that the k-rank k_A is always less than or equal to the rank r_A of **A**, that is:

$$k_A \leq r_A \leq min(I_1, Q) \tag{2.12}$$

Lets consider the set of factor matrices **A**, **B** and **C**, previous defined in Equation (2.5). **A**, **B**, and **C** are unique up to permutation and scaling factors if [17]

$$k_A + k_B + k_C \geq 2Q + 2. \tag{2.13}$$

That is, any matrices $\tilde{\mathbf{A}}$, $\tilde{\mathbf{B}}$, and $\tilde{\mathbf{C}}$ that satisfy (2.5) are connected to **A**, **B**, and **C** as:

$$\tilde{\mathbf{A}} = \mathbf{A}\mathbf{\Pi}\mathbf{\Delta}_1. \tag{2.14}$$

$$\tilde{\mathbf{B}} = \mathbf{B}\mathbf{\Pi}\mathbf{\Delta}_2. \tag{2.15}$$

$$\tilde{\mathbf{C}} = \mathbf{C}\mathbf{\Pi}\mathbf{\Delta}_3. \tag{2.16}$$

where $\mathbf{\Pi}$ is the permutation matrix and $\mathbf{\Delta}_1$, $\mathbf{\Delta}_2$, and $\mathbf{\Delta}_3$ are the diagonal matrices such that

$$\mathbf{\Delta}_1\mathbf{\Delta}_2\mathbf{\Delta}_3 = \mathbf{I}_Q. \tag{2.17}$$

Generalizing, the PARAFAC decomposition of an arbitrary N^{th}-order tensor $\mathcal{X} \in \mathbb{C}^{I_1 \times I_2 \times ... \times I_N}$ can be written in scalar form as

$$x_{i_1,i_2,...,i_N} = \sum_{q=1}^{Q} a^{(1)}_{i_1,q} a^{(2)}_{i_2,q}, ..., a^{(N)}_{i_N,q} = \sum_{q=1}^{Q} \prod_{n=1}^{N} a^{(n)}_{i_n,q}, \tag{2.18}$$

where $a_{i_n,q}$ is the scalar components of the matrix $\mathbf{A}^{I_n \times Q}$. Using the outer product notation, we can write the PARAFAC decomposition as

$$\mathcal{X} = \sum_{q=1}^{Q} \mathbf{A}^{(1)}_{.q} \circ \mathbf{A}^{(2)}_{.q} \circ ... \circ \mathbf{A}^{(N)}_{.q}. \tag{2.19}$$

Nested PARAFAC Decomposition

The Nested PARAFAC model was proposed in [5] and it corresponds to two nested 3^{rd}-order PARAFAC models sharing a common matrix factor. Lets consider an arbitrary 4^{th}-order tensor $\mathcal{X} \in \mathbb{C}^{I_1 \times I_2 \times I_3 \times I_4}$, its Nested PARAFAC decomposition can be written in scalar form as

$$x_{i_1,i_2,i_3,i_4} = \sum_{r_1=1}^{R_1} \sum_{r_2=1}^{R_2} a^{(1)}_{i_1,r_1} b^{(1)}_{i_2,r_1} a^{(2)}_{i_3,r_2} b^{(2)}_{i_4,r_2} g_{r_1,r_2} \tag{2.20}$$

where $a^{(1)}_{i_1,r_1}$, $b^{(1)}_{i_2,r_1}$, $a^{(2)}_{i_3,r_2}$, $b^{(2)}_{i_4,r_2}$, and g_{r_1,r_2} are the scalar components of the matrices $\mathbf{A}^{(1)} \in \mathbb{C}^{I_1 \times R_1}$, $\mathbf{B}^{(1)} \in \mathbb{C}^{I_2 \times R_1}$, $\mathbf{A}^{(2)} \in \mathbb{C}^{I_3 \times R_2}$, $\mathbf{B}^{(2)} \in \mathbb{C}^{I_4 \times R_2}$, and $\mathbf{G} \in \mathbb{C}^{R_1 \times R_2}$, respectively. This tensor decomposition is illustrated on Figure 2.5.

Tucker-3 Decomposition

The Tucker-3 decomposition [25] was proposed in 1966 by L. Tucker. This tensor decomposition represents a tensor $\mathcal{X} \in \mathbb{C}^{I_1 \times I_2 \times I_3}$ in scalar form as

$$x_{i_1,i_2,i_3} = \sum_{p=1}^{P} \sum_{q=1}^{Q} \sum_{r=1}^{R} a_{i_1,p} b_{i_2,q} c_{i_2,r} g_{p,q,r}, \tag{2.21}$$

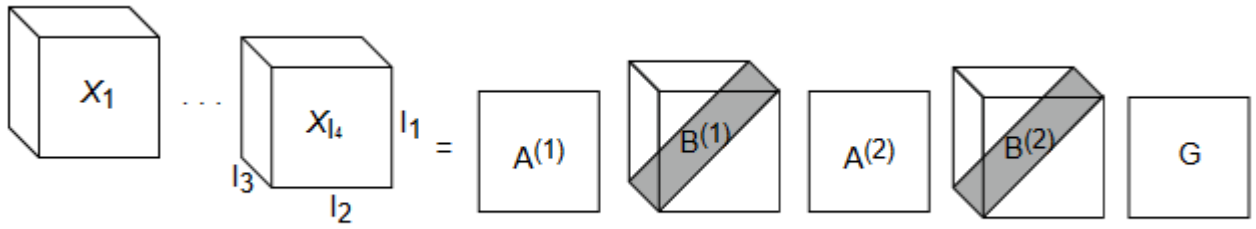

Fig. 2.5: Illustration of the Nested PARAFAC decomposition

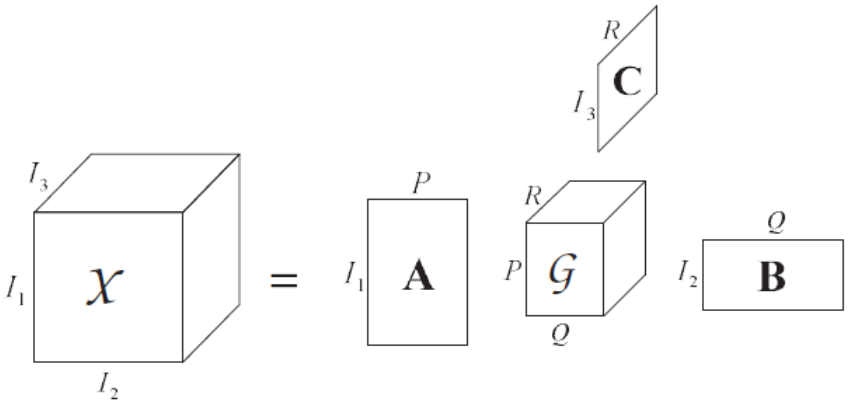

Fig. 2.6: Illustration of the Tucker-3 decomposition. Figure from [24].

where $a_{i_1,p}$, $b_{i_2,q}$ and $c_{i_3,r}$ are the scalar components of the matrices $\mathbf{A}^{I_1 \times P}$, $\mathbf{B}^{I_2 \times Q}$ and $\mathbf{C}^{I_3 \times R}$, respectively, and $g_{p,q,r}$ is a scalar component of the called core tensor $\mathcal{G} \in \mathbb{C}^{P \times Q \times R}$. P, Q, and R are the number of factors in the first, second, and third mode of the tensor. Figure 2.6 illustrates this tensor decomposition. We can see that the Tucker-3 is a decomposition of a 3^{rd}-order tensor and it's not unique, since there exists infinite solutions for the core tensor and the factor matrices that leads to the same tensor $\mathcal{X}$.

There exists two special cases of the Tucker decomposition known by Tucker-2 and Tucker-1 decompositions. Considering the Tucker-3 decomposition showed in (2.21), lets rewrite this equation as

$$x_{i_1,i_2,i_3} = \sum_{p=1}^{P} \sum_{q=1}^{Q} a_{i_1,p} b_{i_2,q} \left(\sum_{r=1}^{R} c_{i_2,r} g_{p,q,r} \right) = \sum_{p=1}^{P} \sum_{q=1}^{Q} a_{i_1,p} b_{i_2,q} h_{p,q,i_3}. \tag{2.22}$$

We can see that (2.22) is the scalar form of the Tucker-2 decomposition, where $c_{i_2,r}$ and $g_{p,q,r}$ form the equivalent core tensor h_{p,q,i_3}. Figure 2.7 illustrates this special case. Now let us rewrite Equation

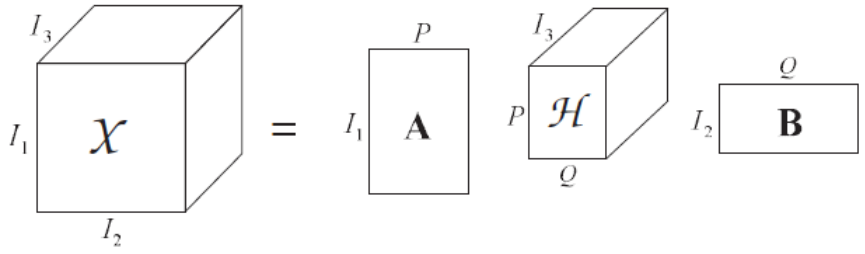

Fig. 2.7: Illustration of the Tucker-2 decomposition. Figure from [24].

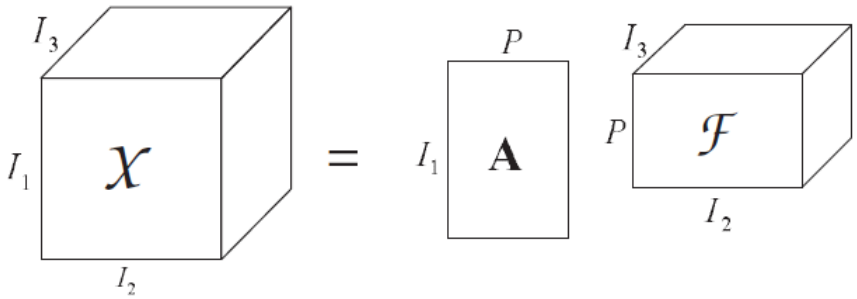

Fig. 2.8: Illustration of the Tucker-1 decomposition. Figure from [24].

(2.21) as

$$x_{i_1,i_2,i_3} = \sum_{p=1}^{P} a_{i_1,p} \left(\sum_{q=1}^{Q} \sum_{r=1}^{R} b_{i_2,q} c_{i_2,r} g_{p,q,r} \right) = \sum_{p=1}^{P} a_{i_1,p} f_{p,i_2,i_3}. \tag{2.23}$$

Equation (2.23) is the scalar form of the Tucker-1 decomposition, where $b_{i_2,q}$, $c_{i_2,r}$, and $g_{p,q,r}$ form the equivalent core tensor f_{p,i_2,i_3}. We can see the illustration of the Tucker-1 decomposition in Figure 2.8.

Generalizing to an arbitrary N^{th}-order tensor $\mathcal{X} \in \mathbb{C}^{I_1 \times I_2 \times \ldots \times I_N}$, the N^{th}-order Tucker decomposition of this tensor is given by

$$x_{i_1,i_2,\ldots,i_N} = \sum_{r_1=1}^{R_1} \sum_{r_2=1}^{R_2} \cdots \sum_{r_N=1}^{R_N} a^{(1)}_{i_1,r_1} a^{(2)}_{i_2,r_2} \ldots a^{(N)}_{i_N,r_N} g_{r_1,r_2,\ldots,r_N}, \tag{2.24}$$

where a_{i_n,r_n} is the scalar component of the matrix $\mathbf{A}^{I_n \times R_n}$ and $g_{r_1,r_2,\ldots,r_N}$ is a scalar component of the N^{th}-order core tensor $\mathcal{G} \in \mathbb{C}^{R_1 \times R_2 \times \ldots \times R_N}$.

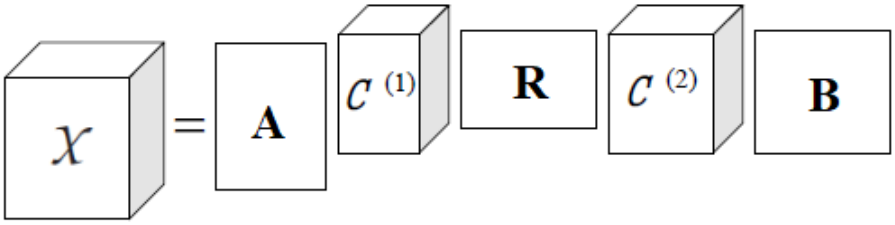

Fig. 2.9: Nested Tucker decomposition for a 4^{th}-order tensor. Figure from [11].

Nested Tucker Decomposition

In this subsection, a tensor decomposition proposed in [11] called Nested Tucker Decomposition (NTD) is presented. For a 4^{th}-order tensor $\mathcal{X} \in \mathbb{C}^{I_1 \times I_2 \times I_3 \times I_4}$, we can write the NTD in scalar form as

$$x_{i_1,i_2,i_3,i_4} = \sum_{r_1=1}^{R_1} \sum_{r_2=1}^{R_2} \sum_{r_3=1}^{R_3} \sum_{r_4=1}^{R_4} a_{i_1,r_1} c^{(1)}_{r_1,i_2,r_2} r_{r_2,r_3} c^{(2)}_{r_3,i_3,r_4} b_{i_4,r_4}, \tag{2.25}$$

where a_{i_1,r_1}, $c^{(1)}_{r_1,i_2,r_2}$, r_{r_2,r_3}, $c^{(2)}_{r_3,i_3,r_4}$, and b_{i_4,r_4} are the scalar components of $\mathbf{A} \in \mathbb{C}^{I_1 \times R_1}$, $\mathcal{C}^{(1)} \in \mathbb{C}^{R_1 \times I_2 \times R_2}$, $\mathbf{R} \in \mathbb{C}^{R_2 \times R_3}$, $\mathcal{C}^{(2)} \in \mathbb{C}^{R_3 \times I_3 \times R_4}$, and $\mathbf{B} \in \mathbb{C}^{I_4 \times R_4}$, respectively. We can see that this decomposition is a concatenation of 3^{rd}-order tensors between three matrices, as illustrated in Figure 2.9. Generalizing this decomposition for an arbitrary N^{th}-order tensor $\mathcal{X} \in \mathbb{C}^{I_1 \times I_2 \times \ldots \times I_N}$, we can write its scalar form as

$$x_{i_1,i_2,\ldots,i_N} = \sum_{r_1=1}^{R_1} \sum_{r_2=1}^{R_2} \ldots \sum_{r_N=1}^{R_N} a^{(1)}_{i_1,r_1} c^{(1)}_{r_1,i_2,r_2} a^{(2)}_{r_2,r_3} c^{(2)}_{r_3,i_3,r_4} \ldots c^{(N-2)}_{r_{2N-5},i_{N-1},r_{2N-4}} a^{(N-1)}_{i_N,r_{2N-4}}, \tag{2.26}$$

where $a^{(1)}_{i_1,r_1}$, $a^{(N-1)}_{i_N,r_{2N-4}}$, $a^{(n+1)}_{r_{2n},r_{2n+1}}$, and $c^{(n)}_{r_{2n-1},i_{n+1},r_{2n}}$ are the scalar components of $\mathbf{A}^{(1)} \in \mathbb{C}^{I_1 \times R_1}$, $\mathbf{A}^{(N-1)} \in \mathbb{C}^{I_N \times R_{2N-4}}$, $\mathbf{A}^{(n+1)} \in \mathbb{C}^{R_{2n} \times R_{2n+1}}$, and $\mathcal{C}^{(n)} \in \mathbb{C}^{R_{2n-1} \times I_{n+1} \times R_{2n}}$, respectively.

2.1.3 *PARATUCK Decomposition*

Once the PARAFAC and Tucker models were presented, it will be presented now a tensor model that shares some features of both models presented before, i.e, this decomposition can be considered as a combination of PARAFAC and TUCKER-2 [17]. This tensor model called PARATUCK was proposed in 1996 by Harshman and Lundy [15]. Consider an arbitrary 3^{rd}-order tensor $\mathcal{X} \in \mathbb{C}^{I \times J \times K}$,

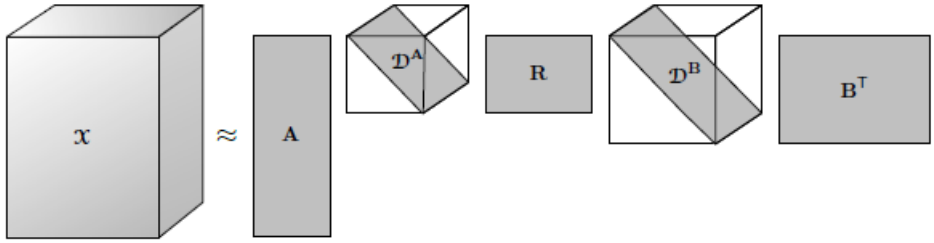

Fig. 2.10: PARATUCK-2 decomposition for a 3^{rd}-order tensor. Figure from [17].

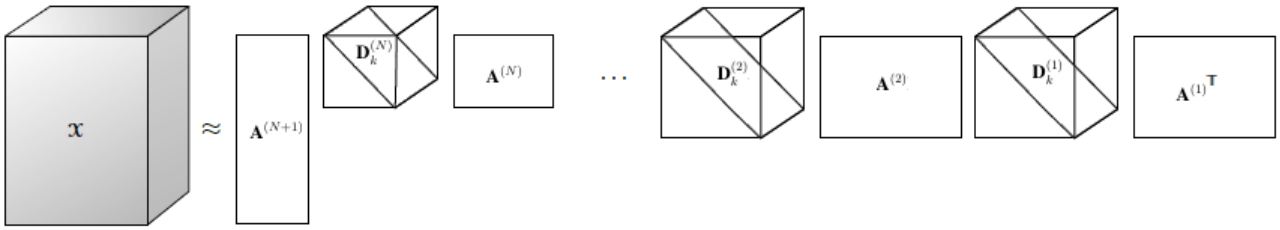

Fig. 2.11: PARATUCK-N decomposition for a 3^{rd}-order tensor. Figure edited from [17].

its PARATUCK-2 decomposition can be written in scalar form as

$$x_{i,j,k} = \sum_{r_2=1}^{R_2} \sum_{r_1=1}^{R_1} a_{i,r_1} d_{k,r_1}^{(a)} r_{r_1,r_2} d_{k,r_2}^{(b)} b_{r_2,j} \tag{2.27}$$

where a_{i,r_1}, $d_{k,r_1}^{(a)}$, r_{r_1,r_2}, $d_{k,r_2}^{(b)}$, and $b_{r_2,j}$ are the scalar components of the matrices $\mathbf{A} \in \mathbb{C}^{I \times R_1}$, $\mathbf{D}^{(A)} \in \mathbb{C}^{K \times R_1}$, $\mathbf{R} \in \mathbb{C}^{R_1 \times R_2}$, $\mathbf{D}^{(B)} \in \mathbb{C}^{K \times R_2}$, and $\mathbf{B}^T \in \mathbb{C}^{R_2 \times J}$. $\mathbf{D}^{(A)}$ and $\mathbf{D}^{(B)}$ are diagonal matrices. We can also express the PARATUCK-2 decomposition in matrix slices terms as

$$\mathbf{X}_{..k} = \mathbf{A}\mathbf{D}_k^{(A)}\mathbf{R}\mathbf{D}_k^{(B)}\mathbf{B}^T. \tag{2.28}$$

This tensor decomposition is illustrated in Figure 2.10.

Generalizing, we can write the PARATUCK-N decomposition of the same arbitrary 3^{rd}-order tensor in matrix slices terms as

$$\mathbf{X}_{..k} = \mathbf{A}^{(N+1)}\mathbf{D}_k^{(N)}\mathbf{A}^{(N)}...\mathbf{D}_k^{(2)}\mathbf{A}^{(2)}\mathbf{D}_k^{(1)}\mathbf{A}^{(1)^T}. \tag{2.29}$$

We can see in Figure 2.11 the illustration of this decomposition.

Coming back to the PARATUCK-2 decomposition, in [15] it was proved the uniqueness for the

general PARATUCK-2 model, considering $\mathbf{D}^{(A)} = \mathbf{D}^{(B)}$, and under the conditions that $R_1 = R_2$ and $\mathbf{R}$ has no zeros. In this case, [15] supposes that there is an alternate representation of $\mathbf{X}_{..k}$ given by

$$\mathbf{X}_{..k} = \tilde{\mathbf{A}}\tilde{\mathbf{D}}_k^{(A)}\tilde{\mathbf{R}}\tilde{\mathbf{D}}_k^{(B)}\tilde{\mathbf{B}}^T. \tag{2.30}$$

where $\tilde{\mathbf{A}}$, $\tilde{\mathbf{D}}_k^{(A)}$, $\tilde{\mathbf{R}}$, $\tilde{\mathbf{D}}_k^{(B)}$, and $\tilde{\mathbf{B}}^T$ have the same size and structural forms of their equivalences in (2.28).

The representations in (2.28) and (2.30) are related as

$$\tilde{\mathbf{A}}(\mathbf{\Pi}_A\mathbf{\Delta}_A) = \mathbf{A}. \tag{2.31}$$

$$\tilde{\mathbf{B}}(\mathbf{\Pi}_B\mathbf{\Delta}_B) = \mathbf{B}. \tag{2.32}$$

$$(\bar{\mathbf{\Delta}}_A\mathbf{\Delta}_A^{-1}\mathbf{\Pi}_A^T)\tilde{\mathbf{R}}(\mathbf{\Pi}_B\mathbf{\Delta}_B^{-1}\bar{\mathbf{\Delta}}_B) = \mathbf{R}, \tag{2.33}$$

and for any $\mathbf{X}_{..k} \neq 0$

$$(z_k\mathbf{\Pi}_A^T)\tilde{\mathbf{D}}_k^{(A)}(\mathbf{\Pi}_A\bar{\mathbf{\Delta}}_A^{-1}) = \mathbf{D}_k^{(A)}. \tag{2.34}$$

$$(z_k^{-1}\mathbf{\Pi}_B^T)\tilde{\mathbf{D}}_k^{(B)}(\mathbf{\Pi}_B\bar{\mathbf{\Delta}}_B^{-1}) = \mathbf{D}_k^{(B)}, \tag{2.35}$$

where $\bar{\mathbf{\Delta}}_{\boldsymbol{A}}$, $\bar{\mathbf{\Delta}}_{\boldsymbol{B}}$, $\mathbf{\Delta}_A$ and $\mathbf{\Delta}_B$ are diagonal matrices, $\mathbf{\Pi}_A$ and $\mathbf{\Pi}_B$ are permutation matrices, and z_k are nonzero scalars.

2.2 Cooperative Communications

In this section, we will introduce the basic concepts of cooperative communications, its system model and its most used communication protocols.

2.2.1 *Introduction to Cooperative Communications*

Aiming to explore the advantages that spatial diversity provides, in cooperative communications, one or more relays are used to help the communication between the source (transmissor) and the destination (receptor). The relay is basically an antenna that will re-transmits the signal from the source to the destination (or to other relay, in case of several relays being used). This scheme helps the direct communication between source and destination, providing some advantages, as, for example, spatial diversity gains, being this the great advantage of cooperative communications [1]. One can see in Figure 2.12 a example of a two-hop cooperative communication, i.e, when is used just a single relay.

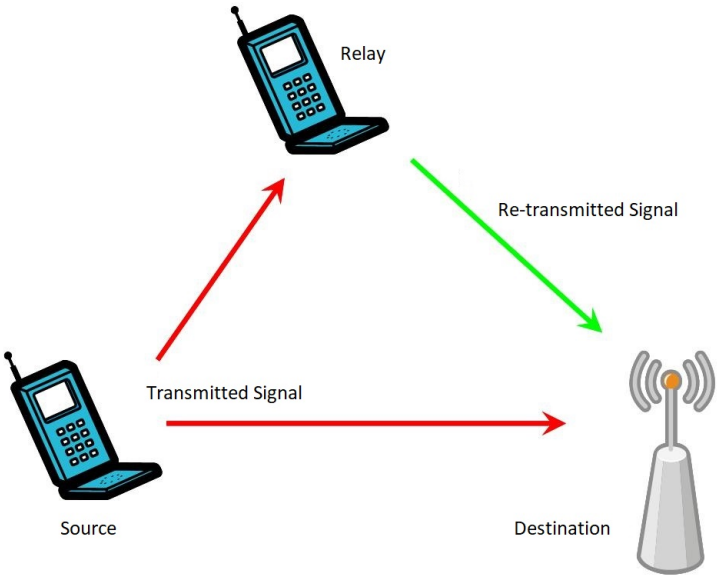

Fig. 2.12: Example of a Cooperative Communication With a Single Relay. Figure From [20].

In cooperative communications there exists several protocols. They can be characterized in two groups:

- Fixed: the resources of the system are divided in a deterministic way between the source and relays. Despite its easy implementation, fixed protocols have the disadvantage of a low bandwidth efficiency. This happens due to the non-efficient resources allocation in the transmission of the relays.

- Adaptive: the resources of the system are not divided in a fixed way between the source and the relays. In this group, there is two main subgroups, selective and incremental. In selective schemes, if the SNR (Signal-to-Noise Ratio) of the received signal at the relay exceeds a determined threshold, the relay re-transmits the data to the destination. However, in case that the channel presences a severe fading, in such way that the SNR of the received signal at the relay is below the determined threshold, the relay does not re-transmits the data. In incremental schemes, if the signal from the source is correctly received by the destination in phase 1 (when the source transmits to the first relay and directly to the destination), there is no need to use the relays, not happening others phases of communication (when the relays transmit to each other and the last one to the destination).

One can tell that the main advantages of cooperative systems, regarding the non-cooperative systems, are the considerable increase in the received power and a best signal quality, due to the spatial

diversity. Also, it provides a better quality of service for edge users. However, some disadvantages are observed, as the increase of interference, data traffic, and the overload of the system [21].

A cooperative communication can be done with a single relay or several relays. Using several relays, they can work in a serial way (multi-hop) or in a parallel. The advantage of using several relays in serial way is the reduced path-loss through the transmission, since the distance between the nodes will be reduced. On the other hand, using several relays in parallel will considerably increase the diversity gains [21]. A cooperative communication using K relays can be done with $K+1$ orthogonal phases, using multiple access techniques as Time Division Multiple Access (TDMA) or Frequency Division Multiple Access (FDMA) [1].

There exists relays that can transmit and receive data at the same time, they are called relays full-duplex, and there exists relays that cannot transmit and receive data at the same time, they are called relays half-duplex. From now on, it will be considered only the use of relays half-duplex.

2.2.2 *Cooperative System Model*

In this subsection, it is considered that there is no direct link between the source and the destination, so the signal received from the destination is only from the relay's channels. Also, it is considered that the relays work in a serial way, i.e, a multi-hop communication, with flat-fading channels.

In phase 1 the source transmits only to the first relay, since there is no direct link between the source and the destination. In the phases 2, 3,..., K the relays communicate with each other, re-transmiting the information signal, and in the phase $K+1$, the last phase, the last relay re-transmits the information signal to the destination.

Let $\mathbf{x} \in \mathbb{C}^{1\times N}$, where N is the number of symbol periods, be the message to be transmitted, $h^{(SR_1)}$ the channel between the source and the first relay and $\mathbf{v}^{(SR_1)} \in \mathbb{C}^{1\times N}$ the Additive White Gaussian Noise (AWGN) in this channel. The received signal by the first relay is given by

$$\mathbf{y}^{(SR_1)} = h^{(SR_1)}\mathbf{x} + \mathbf{v}^{(SR_1)} \in \mathbb{C}^{1\times N}. \tag{2.36}$$

The received signal by the k^{th} relay from the $(k-1)^{th}$ relay, where $k = 2 : K$, is given by

$$\mathbf{y}^{S\ldots(R_{k-1}R_k)} = h^{(R_{k-1}R_k)}Q(\mathbf{y}^{(S\ldots R_{k-1})}) + \mathbf{v}^{(R_{k-1}R_k)} \in \mathbb{C}^{1\times N}, \tag{2.37}$$

where $h^{(R_{k-1}R_k)}$ is the channel between the relays R_{k-1} and R_k, $Q(\cdot)$ is a function that depends on the implemented protocol, $\mathbf{y}^{(S\ldots R_{k-1})} \in \mathbb{C}^{1\times N}$ is the signal received by the relay R_{k-1}, and $\mathbf{v}^{(R_{k-1}R_k)} \in \mathbb{C}^{1\times N}$ is the AWGN present on the channel $\mathbf{h}^{(R_{k-1}R_k)}$.

Finally, the received signal by the destination from the last relay is given by

$$\mathbf{y}^{SR_1...R_KD)} = h^{(R_KD)}Q(\mathbf{y}^{(S...R_K)}) + \mathbf{v}^{(R_KD)} \in \mathbb{C}^{1\times N}, \tag{2.38}$$

where $h^{(R_KD)}$ is the channel between the relay R_K and the destination, $\mathbf{y}^{(S...R_K)} \in \mathbb{C}^{1\times N}$ is the signal received by the relay R_K, and $\mathbf{v}^{(R_KD)} \in \mathbb{C}^{1\times N}$ is the AWGN present on this channel $h^{(R_KD)}$.

2.2.3 *Cooperative Protocols*

As previously described, cooperative protocols can be classified between fixed and adaptive. In this section it will be introduced the most important protocols of each group.

Fixed Protocols

A very popular fixed protocol is the AF, where the relay amplifies the signal received from the source and re-transmits it to the next node. This protocol works in two phases, in phase 1, the relay receives the signal from the source as in (2.36). In the other phases, the relays amplify the received signal from the source (or from the previous relay) and re-transmit it to the destination (or the next relay). There exists several expressions for the relay gain, one of the most used is the so called variable gain, that provides the advantage of controlling the transmitted power by the relay. This gain is given by [32]:

$$\beta_R = \frac{\sqrt{P_R}}{\sqrt{P_S|h^{(R)}|^2 + \sigma^2}}, \tag{2.39}$$

where P_R and P_S are the transmitted power of the relay and the source, respectively, $h^{(R)}$ is the channel between the relay and its previous node (can be the source or another relay), and σ^2 is the variance of the noise present in that channel. The signal received by the destination in the last phase is

$$\mathbf{y}^{(SR_1...R_KD)} = \beta_{R_K} h^{(R_KD)}\mathbf{y}^{(SR_1...R_K)} + \mathbf{v}^{(R_KD)} \in \mathbb{C}^{1\times N}. \tag{2.40}$$

where β_{R_K} is the amplify gain of the relay R_K, $\mathbf{y}^{(SR_1...R_K)}$ is the received signal by this relay, $h^{(R_KD)}$ is the channel between this relay and the destination, and $\mathbf{v}^{(R_KD)}$ is the noise present in that channel.

Another very used protocol is the fixed DF, where the relay decodes the received signal, re-encodes, and re-transmits it. Despite the advantage of the fixed DF over the fixed AF in reducing the AWGN effects in the received signal by the destination, there is the disadvantage of sending erroneous signals to the destination, decreasing the performance of the system [1]. The signal received by the first relay in phase 1 is given by Equation (2.36). In the other phases, the relays decode the received signal, re-encode and re-transmit it to the next node, this way, the received signal by the

destination in the last phase is given by

$$\mathbf{y}^{(SR_1 \ldots R_K D)} = h^{(R_K D)} \mathbf{y}_*^{(SR_1 \ldots R_K)} + \mathbf{v}^{(R_K D)} \in \mathbb{C}^{1 \times N}. \tag{2.41}$$

where $\mathbf{y}_*^{(SR_1 \ldots R_K)}$ is the signal $\mathbf{y}^{(SR_1 \ldots R_K)}$ decoded and re-encoded.

There are others fixed protocols that are not so popular as the two previously described. However, it is worth to cite the protocol CF, where the relays re-transmits a quantized and compressed version of the received signal by it. Another protocol is the Coded Cooperation, where the relay adds some redundancy in the signal, aiming recover the original information in case of propagation errors during the transmission.

Adaptive Protocols

As previously discussed, fixed protocols suffer with low efficiency in bandwidth, causing a considerably loss in transmission rate. Aiming eliminate this disadvantage, the adaptive protocols were developed, the most popular one being the selective Decode-and-Forward, or selective DF [1].

In selective DF, the relay only decodes, re-encodes and re-transmits the data to the next node if the instantaneous SNR of the channel between the relay and the previous node is above a determined threshold. Otherwise, i.e, if the instantaneous SNR of this channel is under the determined threshold, the relay does not re-transmit to the next node. In this case, the relay idles. The received signal by the destination re-transmitted by the last relay is given by

$$\mathbf{y}^{(SR_1 \ldots R_K D)} = \begin{cases} h^{(R_K D)} \mathbf{y}_*^{(SR_1 \ldots R_K)} + \mathbf{v}^{(R_K D)}, & \text{if} \quad |h^{(R_{K-1} R_K)}|^2 \geq G \\ 0, & \text{if} \quad |h^{(R_{K-1} R_K)}|^2 < G. \end{cases} \tag{2.42}$$

where G is the threshold.

Another adaptive protocol is the Incremental Relaying. In this protocol the destination sends the information to the relays telling if the signal from the source was or not correctly received. If the signal was correctly received, the relays do not need to work. But if the signal was not correctly received by the destination, the relays will use any fixed protocol to work on. The Incremental Relaying has a better spectral efficiency if compared to the fixed protocols previously described, as in this protocol the relay does not need to work every time [1].

2.3 MIMO

2.3.1 *Introduction to MIMO Systems*

Wireless communication systems that use a single transmit and receive antenna are called Single-Input Single-Output (SISO) systems, whereas systems that use a single transmit and multiple receive antennas are called Single-Input Multiple-Output (SIMO) systems, and systems using multiple transmit and a single receive antenna are called Multiple-Input Single-Output (MISO) systems. The goal of this subsection is to discuss about systems that use multiple transmit and multiple receive antennas, called MIMO systems.

This wireless networking technology considerably improves the range and the capacity of wireless communication systems. Also, it poses new challenges for digital signal processing, since the processing algorithms become more complex when multiple antennas at both ends of the communication channel are used [2].

MIMO systems can exploit both the diversity and the multiplexing gain [2]. However, it is not possible to exploit both maximum diversity and maximum multiplexing gain at the same time [33].

The most important advantages of multiple antenna systems are [2]:

- Interference reduction: in MIMO systems it is possible to separate the signals with different spatial signatures, decreasing, this way, the co-channel interference. In order to achieve this interference reduction, it is necessary some knowledge of the channel.

- Diversity gain: due to the multiple antennas at both ends, potential diversity gains are provided in MIMO systems. Diversity gain is proportional to the number of independent channels in the system. Higher the diversity gain, lower is the probability of error. Also, the diversity gain tell us how fast this probability of error is decreasing as the SNR increases.

- Multiplexing gain: multiplexing gain is also a benefit of the using of multiple antennas at both ends of the communication system. In MIMO systems that have a rich scattering environment, several communication channels in the same frequency band can be used.

We can see in Figure 2.13 a point-to-point MIMO system with M_t transmit antennas and M_r receive antennas, leading then, to $M_t M_r$ communication channels.

We can represent this system based on the following discrete time model [22]:

$$\begin{bmatrix} y_1 \\ \vdots \\ y_{M_r} \end{bmatrix} = \begin{bmatrix} h_1 \dots h_{1M_t} \\ \vdots \ddots \vdots \\ h_{M_r} \dots h_{M_r M_t} \end{bmatrix} \begin{bmatrix} x_1 \\ \vdots \\ x_{M_t} \end{bmatrix} + \begin{bmatrix} v_1 \\ \vdots \\ v_{M_r} \end{bmatrix}, \tag{2.43}$$

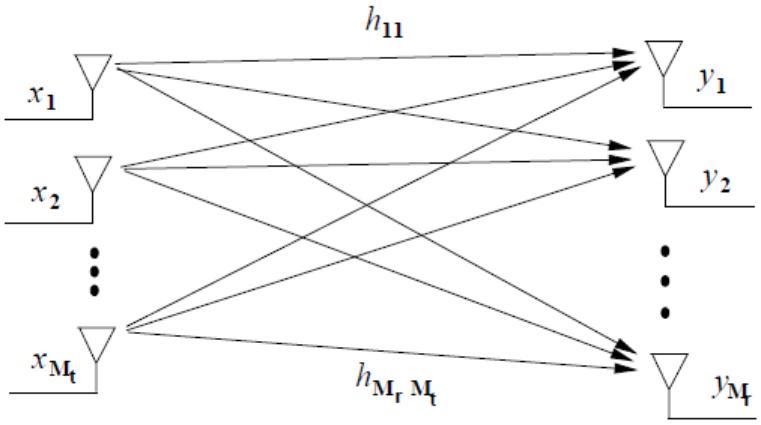

Fig. 2.13: An example of a MIMO system. Figure from [22].

where y_i and v_i, for $i = 1, ..., M_r$ are the received signal and the noise for each received antenna, respectively, x_j, for $j = 1, ..., M_t$ are the transmitted symbols for each transmitting antenna, and h_{ij} are the channels from each transmitting antenna to each received antenna. In other words

$$\mathbf{y} = \mathbf{H}\mathbf{x} + \mathbf{v}, \tag{2.44}$$

where $\mathbf{x} \in \mathbb{C}^{M_t \times 1}$ is the transmitted symbols vector, $\mathbf{v} \in \mathbb{C}^{M_r \times 1}$ is the AWGN vector, and $\mathbf{H} \in \mathbb{C}^{M_r \times M_t}$ is the matrix of channel gains from the transmit antenna to the receive antenna.

One can made some assumptions about the knowledge of the channel matrix $\mathbf{H}$ at the transmitter, called Channel Side Information at the Transmitter (CSIT), and the receiver, called Channel Side Information at the Receiver (CSIR). CSIR is assumed by sending a pilot sequence for channel estimation. In case of an available feedback channel, CSIR is sent back to the transmitter, providing CSIT (that can also be available by exploiting some properties of propagation in time-division duplexing, no needing an available feedback channel).

2.3.2 *MIMO Cooperative Systems*

In MIMO cooperative systems, all the nodes have multiple antennas, providing more spatial diversity gains (distributed spatial diversity due to the relays and a concentrated spatial diversity due to the multiple antennas in all nodes). Figure 2.13 illustrates a MIMO cooperative system using a single relay. For a MIMO cooperative system using a single relay, as illustrated in Figure 2.13, the signal received by each antenna at the destination node, using a AF protocol with a fixed gain, for example,

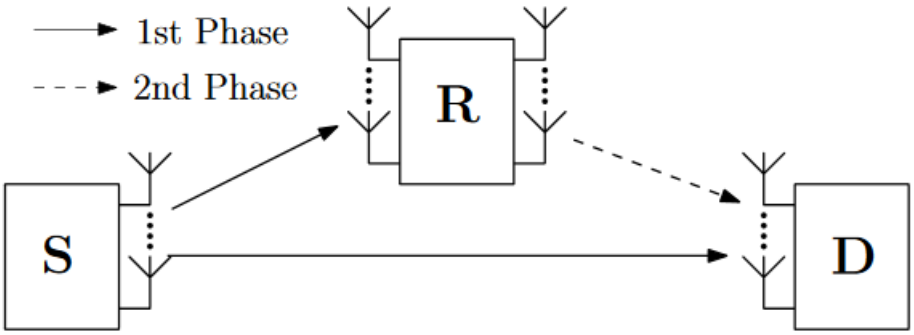

Fig. 2.14: An example of MIMO cooperative system with a single relay. Figure from [28].

is given by

$$\begin{bmatrix} y_1^{(SRD)} \\ \vdots \\ y_{M_r}^{(SRD)} \end{bmatrix} = \begin{bmatrix} h_1^{(RD)} \dots h_{1M_k}^{(RD)} \\ \vdots \ddots \vdots \\ h_{M_r}^{(RD)} \dots h_{M_rM_k}^{(RD)} \end{bmatrix} \begin{bmatrix} \beta y_1^{(SR)} \\ \vdots \\ \beta y_{M_k}^{(SR)} \end{bmatrix} + \begin{bmatrix} v_1^{(RD)} \\ \vdots \\ v_{M_r}^{(RD)} \end{bmatrix}, \tag{2.45}$$

where $y_i^{(SRD)}$ and $v_i^{(RD)}$, for $i = 1, ..., M_r$ are the received signal and the noise for each received antenna, respectively, y_j, for $j = 1, ..., M_k$ are the received signal by the relay from the source for each transmitting antenna, and h_{ij} are the relay-destination channels from each transmitting antenna to each received antenna. In other words

$$\mathbf{y}^{(SRD)} = \mathbf{H}^{(RD)} \beta \mathbf{y}^{(SR)} + \mathbf{v}^{(RD)}, \tag{2.46}$$

where $\mathbf{v}^{(RD)} \in \mathbb{C}^{M_r \times 1}$ is the AWGN vector, $\mathbf{H}^{(RD)} \in \mathbb{C}^{M_r \times M_k}$ is the matrix of channel gains from the relay to the destination, β is the fixed gain, and $\mathbf{y}^{(SR)} \in \mathbb{C}^{M_k \times 1}$ is the signal received by the relay given by

$$\begin{bmatrix} y_1^{(SR)} \\ \vdots \\ y_{M_k}^{(SR)} \end{bmatrix} = \begin{bmatrix} h_1^{(SR)} \dots h_{1M_t}^{(SR)} \\ \vdots \ddots \vdots \\ h_{M_k}^{(SR)} \dots h_{M_kM_t}^{(SR)} \end{bmatrix} \begin{bmatrix} x_1 \\ \vdots \\ x_{M_t} \end{bmatrix} + \begin{bmatrix} v_1^{(SR)} \\ \vdots \\ v_{M_k}^{(SR)} \end{bmatrix}, \tag{2.47}$$

in other words

$$\mathbf{y}^{(SR)} = \mathbf{H}^{(SR)} \mathbf{x} + \mathbf{v}^{(SR)}, \tag{2.48}$$

where $\mathbf{x} \in \mathbb{C}^{M_t \times 1}$ is the transmitted symbol, $\mathbf{v}^{(SR)} \in \mathbb{C}^{M_k \times 1}$ is the AWGN vector, and $\mathbf{H} \in \mathbb{C}^{M_k \times M_t}$ is the matrix of channel gains from the source to the relay. M_t, M_k and M_r are the number of antennas in the source, relay and destination nodes, respectively.

Chapter 3

PROPOSED PARATUCK-N SEMI-BLIND RECEIVERS

This chapter has three sections, the first one is a bibliography review of some works that use tensor decompositions applied in wireless communication systems. The second section presents the multi-hop MIMO AF cooperative system model used in this work. In the third section we present the proposed non-iterative semi-blind algorithms based on the Kronecker product and on the PARATUCK-N model, for jointly estimating the symbols and the channels.

3.1 Bibliography Review

Due to its advantages in exploring the multidimensional nature of a problem, tensor decompositions are applied in several areas, including digital signal processing [3], [4], [5] and telecommunications [6], [7], [8]. In particular, tensor analysis has also shown to be an efficient approach for channel and/or symbol estimation in cooperative MIMO systems [9], [10], [11], [12], [13].

In [9] three semi-blind receivers in a two-hop MIMO AF relaying system using the KRST coding were proposed, this system model is shown in the Figure 3.1. These receivers combine two tensor models (PARAFAC and PARATUCK-2), that enables the joint estimation of the symbols and the channels of the source-relay and relay-destination links. One of these methods is a PARATUCK-2 Alternating Least Squares (ALS)-based receiver where the link source-destination is not used, so the symbol and channel estimation is based only on the source-relay-destination link. The other two receivers are also ALS-based receivers, called Sequential PARAFAC/PARATUCK2 and Combined PARAFAC/PARATUCK2, they used an ALS-based estimation at the relay assisted link and a Singular-Value Decomposition (SVD) at the direct link. The tensor modeling of this work is similar to the one described in the Subsection 3.2.1, but with the addition of the direct link SD. The present

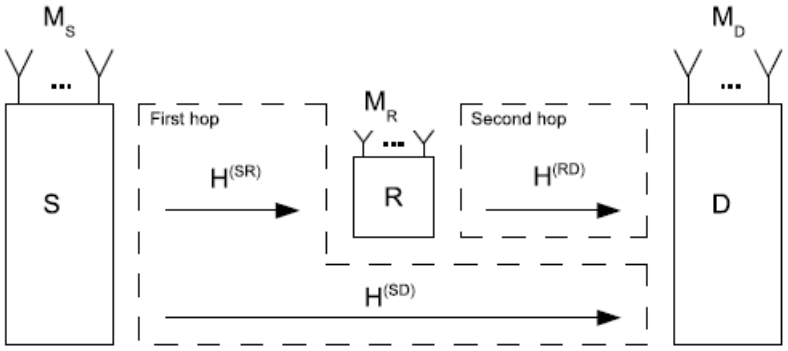

Fig. 3.1: A two-hop MIMO AF cooperative system. Figure from [9].

dissertation generalizes the tensor modeling of [9] for the multi-hop case, but without the direct link.

Also in a two-hop MIMO AF relaying system, in [10] a Nested-PARAFAC tensor model is formulated and two iterative semi-blind receivers are proposed, for jointly estimating the symbol and the channels of the communication links. A fourth-order tensor $\mathcal{X} \in \mathbb{C}^{I_1 \times I_2 \times I_3 \times I_4}$ was used, and its Nested-PARAFAC decomposition is given by

$$x_{i_1,i_2,i_3,i_4} = \sum_{r_1=1}^{R_1} \sum_{r_2=1}^{R_2} b^{(1)}_{i_1,r_1} b^{(2)}_{i_2,r_1} u_{r_1,r_2} d^{(1)}_{i_3,r_2} d^{(2)}_{i_4,r_2} \tag{3.1}$$

where $\mathbf{U} \in \mathbb{C}^{R_1 \times R_2}$ is the core matrix, and $\mathbf{B}^{(i)} \in \mathbb{C}^{I_i \times R_1}$ for $i = \{1, 2\}$ and $\mathbf{D}^{(j)} \in \mathbb{C}^{I_j \times R_2}$ for $j = \{1, 2\}$ are the factor matrices.

There are other works that exploit tensor approches in MIMO systems, as [12], where a Tensor Space-Time (TST) coding is used in MIMO wireless communication systems, and in [11], where this TST coding is used to induce a Nested Tucker decomposition in a MIMO relaying system. The Nested Tucker decomposition is based on tensor train decomposition [34] [35]. This proposed TST coding allows spreading and multiplexing the transmitted symbols in both space (transmit antennas) and time (chips and blocks) domains [12].

Regarding the PARATUCK tensor model, a blind receiver based on a generalized 4^{th}-order PARATUCK-2 decomposition is proposed in [13] for Space-Time Frequency (STF) MIMO systems with spreading multiplexing. This blind receiver jointly estimate the symbol, channel, and code matrices, using the Levenberg-Marquardt algorithm. In this tensor model, the core tensor of the PARATUCK-2 decomposition is a spatial coding matrix combined with two 3^{rd}-order tensors.

In [23], the PARATUCK-2 decomposition is used for a space-time spreading-multiplexing in MIMO wireless communication systems. In [29], a new tensor space-time-frequency coding structure has been proposed for MIMO Orthogonal Frequency Division Multiplexing - Code Division

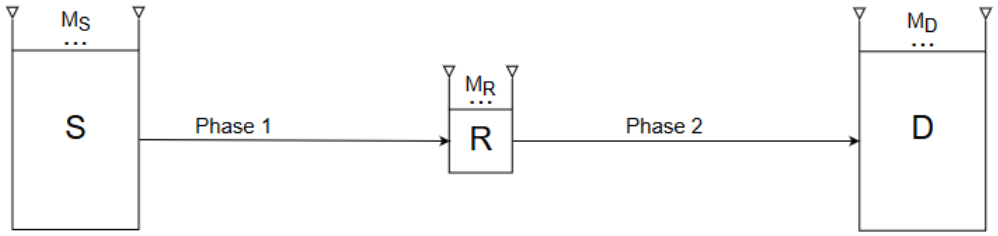

Fig. 3.2: MIMO cooperative system model with 1 relay.

Multiple Access (OFDM-CDMA) wireless communication systems. Two new tensor models called generalized PARATUCK-(N_1,N) and Tucker-(N_1,N) are proposed. Also, in this work are proposed two semi-blind receivers for jointly estimate the channel and symbols matrices. The first receiver is based on a ALS algorithm, while the second one is based on the least squares estimation of the Kronecker product matrix.

In the next section the system models used in the present work will be presented, i.e, the two- three- and multi-hop systems.

3.2 System Model

3.2.1 *Case of 1 Relay (Two-Hop System)*

For the case using a single relay, it is considered a two-hop one-way cooperative MIMO AF relay system, with one source (S) node, one destination (D) node and one relay (R) node, as illustrated in Figure 3.2, where M_X denotes the number of antennas at node X (e.g, M_S denotes the number of antennas at node S). All the channels are assumed to be invariant during the total transmission time and to undergo frequency flat fading. The transmitted symbols are Quadrature Amplitude Modulation (QAM)-modulated or Phase Shift Keying (PSK)-modulated. The relay is half-duplex and the transmission runs in two phases. In phase 1 the source transmits to the relay, while in phase 2 the relay transmits to the destination.

Consider that $\mathbf{H}^{(SR)} \in \mathbb{C}^{M_R \times M_S}$ and $\mathbf{H}^{(RD)} \in \mathbb{C}^{M_D \times M_R}$ are MIMO channel matrices of the source-relay and the relay-destination links, respectively. $\mathbf{S} \in \mathbb{C}^{N \times M_S}$ is the matrix with the information symbols multiplexed to the M_S antennas during N consecutive symbol periods. A simplified KRST coding [14] is used at the source to introduce time redundancy:

$$\mathbf{X}_{..p} = D_p(\mathbf{G}_0)\mathbf{S}^T \in \mathbb{C}^{M_S \times N} \tag{3.2}$$

where $p = 1, ..., P$, $\mathbf{X}_{..p}$ is the transmitted signal matrix at the p^{th} transmission block, $\mathbf{G}_0 \in \mathbb{C}^{P \times M_S}$ is the coding matrix of the source node, and P is the number of transmission blocks. The matrix with the signals received by the relay R during the p^{th} transmission block is given by

$$\tilde{\mathbf{Y}}_{..p}^{(SR)} = \mathbf{H}^{(SR)}\mathbf{X}_{..p} + \mathbf{V}_{..p}^{(SR)} \in \mathbb{C}^{M_R \times N}, \tag{3.3}$$

where $\mathbf{V}_{..p}^{(SR)} \in \mathbb{C}^{M_R \times N}$ is the AWGN matrix during the p^{th} transmission block in the SR link. Considering $\mathbf{G}_1 \in \mathbb{C}^{P \times M_R}$ as the coding matrix (or gain matrix) of the AF relay, the amplified signal $D_p(\mathbf{G}_1)\tilde{\mathbf{Y}}_{..p}^{(SR)} \in \mathbb{C}^{M_R \times N}$ is transmitted by the relay R to the destination.

The matrix with the signals received by the destination during the p^{th} transmission block is

$$\tilde{\mathbf{Y}}_{..p}^{(SRD)} = \mathbf{H}^{(RD)} D_p(\mathbf{G}_1)\tilde{\mathbf{Y}}_{..p}^{(SR)} + \mathbf{V}_{..p}^{(RD)} \in \mathbb{C}^{M_D \times N}, \tag{3.4}$$

where $\mathbf{V}_{..p}^{(RD)} \in \mathbb{C}^{M_D \times N}$ is the noise matrix during the p^{th} transmission block in the RD link.

Substituting (3.2) and (3.3) into (3.4), we get:

$$\tilde{\mathbf{Y}}_{..p}^{(SRD)} = \mathbf{H}^{(RD)} D_p(\mathbf{G}_1)\mathbf{H}^{(SR)} D_p(\mathbf{G}_0)\mathbf{S}^T + \mathbf{H}^{(RD)} D_p(\mathbf{G}_1)\mathbf{V}_{..p}^{(SR)} + \mathbf{V}_{..p}^{(RD)} \in \mathbb{C}^{M_D \times N}. \tag{3.5}$$

In other words

$$\tilde{\mathbf{Y}}_{..p}^{(SRD)} = \mathbf{Y}_{..p}^{(SRD)} + \mathbf{V}_{..p}^{(SRD)} \in \mathbb{C}^{M_D \times N}, \tag{3.6}$$

where $\mathbf{Y}_{..p}^{(SRD)}$ is the noiseless signal given by

$$\mathbf{Y}_{..p}^{(SR_1R_2D)} = \mathbf{H}^{(RD)} D_p(\mathbf{G}_1)\mathbf{H}^{(SR)} D_p(\mathbf{G}_0)\mathbf{S}^T \in \mathbb{C}^{M_D \times N}, \tag{3.7}$$

and $\mathbf{V}_{..p}^{(SRD)}$ is the global noise given by

$$\mathbf{V}_{..p}^{(SRD)} = \mathbf{H}^{(RD)} D_p(\mathbf{G}_1)\mathbf{V}_{..p}^{(SR)} + \mathbf{V}_{..p}^{(RD)} \in \mathbb{C}^{M_D \times N}. \tag{3.8}$$

Equation (3.7) corresponds to a PARATUCK-2 decomposition [15] that can be rewritten in scalar form as

$$y_{m_D,n,p}^{(SRD)} = \sum_{m_R=1}^{M_R} \sum_{m_S=1}^{M_S} h_{m_D,m_R}^{(RD)} g_{p,m_R}^{(1)} h_{m_R,m_S}^{(SR)} g_{p,m_S}^{(0)} s_{n,m_S}. \tag{3.9}$$

3.2.2 *Case of 2 Relays (Three-Hop System)*

For the case using 2 relays, it is considered a three-hop one-way cooperative MIMO AF relay system, with one source (S) node, one destination (D) node and two relays (R_1 and R_2) nodes, as

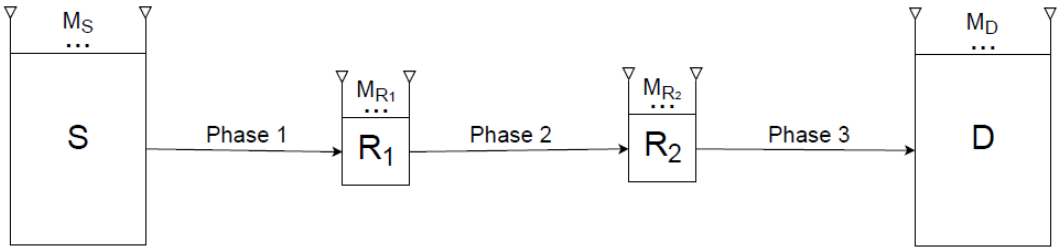

Fig. 3.3: MIMO cooperative system model with 2 relays.

illustrated in Figure 3.3, where M_X denotes the number of antennas at node X (e.g, M_S denotes the number of antennas at node S). Similarly as in Subsection 3.2.1, all the channels are assumed to be invariant during the total transmission time and to undergo frequency flat fading. The relay is half-duplex and the transmission runs in three phases. In the first phase the source transmits to the first relay, while in the second phase the first relay transmits to the second relay, and finally, in the third phase the second relay transmits to the destination.

Consider that $\mathbf{H}^{(SR_1)} \in \mathbb{C}^{M_{R_1} \times M_S}$, $\mathbf{H}^{(R_1R_2)} \in \mathbb{C}^{M_{R_2} \times M_{R_1}}$ and $\mathbf{H}^{(R_2D)} \in \mathbb{C}^{M_D \times M_{R_2}}$ are MIMO channel matrices of the source-relay[1], relay[1]-relay[2] and the relay[2]-destination links, respectively. $\mathbf{S} \in \mathbb{C}^{N \times M_S}$ is the matrix with the information symbols multiplexed to the M_S antennas during N consecutive symbol periods. The same codification in (3.2) is used in this scenario. Similarly as in (3.3), the matrix with the signals received by the relay R_1 during the p^{th} transmission block is given by

$$\tilde{\mathbf{Y}}_{..p}^{(SR_1)} = \mathbf{H}^{(SR_1)}\mathbf{X}_{..p} + \mathbf{V}_{..p}^{(SR_1)} \in \mathbb{C}^{M_{R_1} \times N}, \tag{3.10}$$

where $\mathbf{V}_{..p}^{(SR_1)} \in \mathbb{C}^{M_{R_1} \times N}$ is the AWGN matrix during the p^{th} transmission block in the SR_1 link. Considering $\mathbf{G}_1 \in \mathbb{C}^{P \times M_{R_1}}$ as the coding matrix (or gain matrix) of the AF relay[1], the amplified signal $D_p(\mathbf{G}_1)\tilde{\mathbf{Y}}_{..p}^{(SR_1)} \in \mathbb{C}^{M_{R_1} \times N}$ is transmitted by the relay R_1 to the relay R_2.

Similarly in (3.4), the matrix with the signals received by the relay R_2 during the p^{th} transmission block can then be written as

$$\tilde{\mathbf{Y}}_{..p}^{(SR_1R_2)} = \mathbf{H}^{(R_1R_2)} D_p(\mathbf{G}_1)\tilde{\mathbf{Y}}_{..p}^{(SR_1)} + \mathbf{V}_{..p}^{(R_1R_2)} \in \mathbb{C}^{M_{R_2} \times N}. \tag{3.11}$$

where $\mathbf{V}_{..p}^{(R_1R_2)} \in \mathbb{C}^{M_{R_2} \times N}$ is the noise matrix during the p^{th} transmission block in the R_1R_2 link. Then, considering $\mathbf{G}_2 \in \mathbb{C}^{P \times M_{R_2}}$ as the coding matrix (or gain matrix) of the AF relay[2], the amplified signal $D_p(\mathbf{G}_2)\tilde{\mathbf{Y}}_{..p}^{(SR_1R_2)}$ is transmitted by the relay R_2 to the destination.

Finally, we have that the signal received by the destination during the p^{th} transmission block is

$$\tilde{\mathbf{Y}}_{..p}^{(SR_1R_2D)} = \mathbf{H}^{(R_2D)} D_p(\mathbf{G}_2)\tilde{\mathbf{Y}}_{..p}^{(SR_1R_2)} + \mathbf{V}_{..p}^{(R_2D)} \in \mathbb{C}^{M_D \times N}, \tag{3.12}$$

where $\mathbf{V}_{..p}^{(R_2D)} \in \mathbb{C}^{M_D \times N}$ is the noise matrix during the p^{th} transmission block in the R_2D link.

Substituting (3.2), (3.10) and (3.11) into (3.12), we get:

$$\tilde{\mathbf{Y}}_{..p}^{(SR_1R_2D)} = \mathbf{H}^{(R_2D)} D_p(\mathbf{G}_2)\mathbf{H}^{(R_1R_2)} D_p(\mathbf{G}_1)\mathbf{H}^{(SR_1)} D_p(\mathbf{G}_0)\mathbf{S}^T + \mathbf{H}^{(R_2D)} D_p(\mathbf{G}_2)\mathbf{H}^{(R_1R_2)} D_p(\mathbf{G}_1)\mathbf{V}_{..p}^{(SR_1)} + \mathbf{H}^{(R_2D)} D_p(\mathbf{G}_2)\mathbf{V}_{..p}^{(R_1R_2)} + \mathbf{V}_{..p}^{(R_2D)} \in \mathbb{C}^{M_D \times N}. \quad (3.13)$$

In other words

$$\tilde{\mathbf{Y}}_{..p}^{(SR_1R_2D)} = \mathbf{Y}_{..p}^{(SR_1R_2D)} + \mathbf{V}_{..p}^{(SR_1R_2D)} \in \mathbb{C}^{M_D \times N}, \quad (3.14)$$

where $\mathbf{Y}_{..p}^{(SR_1R_2D)}$ is the noiseless signal given by

$$\mathbf{Y}_{..p}^{(SR_1R_2D)} = \mathbf{H}^{(R_2D)} D_p(\mathbf{G}_2)\mathbf{H}^{(R_1R_2)} D_p(\mathbf{G}_1)\mathbf{H}^{(SR_1)} D_p(\mathbf{G}_0)\mathbf{S}^T \in \mathbb{C}^{M_D \times N}, \quad (3.15)$$

and $\mathbf{V}_{..p}^{(SR_1R_2D)}$ is the global noise given by

$$\mathbf{V}_{..p}^{(SR_1R_2D)} = \mathbf{H}^{(R_2D)} D_p(\mathbf{G}_2)\mathbf{H}^{(R_1R_2)} D_p(\mathbf{G}_1)\mathbf{V}_{..p}^{(SR_1)} + \mathbf{H}^{(R_2D)} D_p(\mathbf{G}_2)\mathbf{V}_{..p}^{(R_1R_2)} + \mathbf{V}_{..p}^{(R_2D)} \in \mathbb{C}^{M_D \times N}. \quad (3.16)$$

Equation (3.15) corresponds to a PARATUCK-3 decomposition [15] that can be rewritten in scalar form as

$$y_{m_D,n,p}^{(SR_1R_2D)} = \sum_{m_{R_2}=1}^{M_{R_2}} \sum_{m_{R_1}=1}^{M_{R_1}} \sum_{m_S=1}^{M_S} h_{m_D,m_{R_2}}^{(R_2D)} g_{p,m_{R_2}}^{(2)} h_{m_{R_2},m_{R_1}}^{(R_1R_2)} g_{p,m_{R_1}}^{(1)} h_{m_{R_1},m_S}^{(SR_1)} g_{p,m_S}^{(0)} s_{n,m_S}. \quad (3.17)$$

3.2.3 *Case of K Relays ((K+1)-Hop System)*

In the present subsection, it is considered a $(K+1)$-hop one-way cooperative MIMO AF relay system, with one source (S) node, one destination (D) node and K relays (R_1, R_2, ..., R_K) nodes, as illustrated in Figure 3.4, where M_X denotes the number of antennas at node X (e.g, M_S denotes the number of antennas at node S). All the assumptions here will be the same as in the previous subsections. The transmission runs in $K+1$ phases. In the first phase, the first relay transmits to the second relay, in the second phase the second relay transmits to the third relay, and so on, until the K^{th} relay (the last one) transmits to the destination in the $(K+1)^{th}$ phase.

Consider that $\mathbf{H}^{(SR_1)} \in \mathbb{C}^{M_{R_1} \times M_S}$, $\mathbf{H}^{(R_{k-1}R_k)} \in \mathbb{C}^{M_{R_k} \times M_{R_{k-1}}}$ and $\mathbf{H}^{(R_KD)} \in \mathbb{C}^{M_D \times M_{R_K}}$ are MIMO channel matrices of the source-relay[1], relay^{k-1}-relay^k and the relay^K-destination links, respectively, for $k = 2, ...K$. The same codification in (3.2) is used in this scenario, leading to (3.3), as in the previous subsections. This process repeats for the K relays.

Considering $\mathbf{G}_{k-1} \in \mathbb{C}^{P \times M_{R_{k-1}}}$ as the coding matrix (or gain matrix) of the relay^{k-1}, the amplified

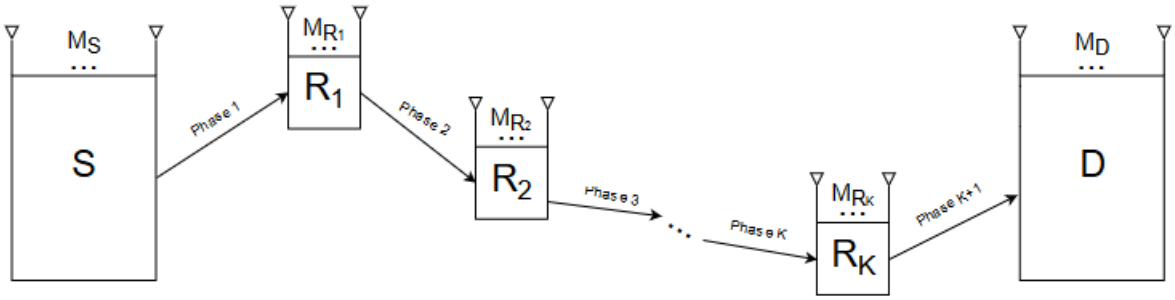

Fig. 3.4: MIMO cooperative system model with K relays.

signal $D_p(\mathbf{G}_{k-1})\tilde{\mathbf{Y}}_{..p}^{(S...R_{k-1})} \in \mathbb{C}^{M_{R_{k-1}} \times N}$ is transmitted by the relay R_{k-1} to the relay R_k, for $k = 2, ..., K$.

The signal received by the relay R_k during the p^{th} transmission block can then be written as

$$\tilde{\mathbf{Y}}_{..p}^{(SR_1...R_k)} = \mathbf{H}^{(R_{k-1}R_k)} D_p(\mathbf{G}_{k-1}) \tilde{\mathbf{Y}}_{..p}^{(SR_1...R_{k-1})} + \mathbf{V}_{..p}^{(R_{k-1}R_k)} \in \mathbb{C}^{M_{R_k} \times N}. \tag{3.18}$$

where $\mathbf{V}_{..p}^{(R_{k-1}R_k)} \in \mathbb{C}^{M_{R_k} \times N}$ is the noise matrix during the p^{th} transmission block in the $R_{k-1}R_k$ link. Then, considering $\mathbf{G}_K \in \mathbb{C}^{P \times M_{R_K}}$ as the coding matrix (or gain matrix) of the relay^K, the amplified signal $D_p(\mathbf{G}_K)\tilde{\mathbf{Y}}_{..p}^{(SR_1...R_K)}$ is transmitted by the relay R_K to the destination.

Finally, we have that the signal received by the destination during the p^{th} transmission block is

$$\tilde{\mathbf{Y}}_{..p}^{(SR_1...R_KD)} = \mathbf{H}^{(R_KD)} D_p(\mathbf{G}_K) \tilde{\mathbf{Y}}_{..p}^{(SR_1...R_K)} + \mathbf{V}_{..p}^{(R_KD)} \in \mathbb{C}^{M_D \times N}, \tag{3.19}$$

where $\mathbf{V}_{..p}^{(R_KD)} \in \mathbb{C}^{M_D \times N}$ is the noise matrix during the p^{th} transmission block in the R_KD link.

We can summarize (3.19) as:

$$\tilde{\mathbf{Y}}_{..p}^{(SR_1...R_KD)} = \mathbf{Y}_{..p}^{(SR_1...R_KD)} + \mathbf{V}_{..p}^{(SR_1...R_KD)} \in \mathbb{C}^{M_D \times N}, \tag{3.20}$$

where $\mathbf{Y}_{..p}^{(SR_1...R_KD)}$ is the noiseless signal given by

$$\mathbf{Y}_{..p}^{(SR_1...R_KD)} = \mathbf{H}^{(R_KD)} D_p(\mathbf{G}_K) \mathbf{H}^{(R_{K-1}R_K)} D_p(\mathbf{G}_{K-1}) ... \mathbf{H}^{(SR_1)} D_p(\mathbf{G}_0) \mathbf{S}^T \in \mathbb{C}^{M_D \times N}, \tag{3.21}$$

which can be written in a recursively way as

$$\mathbf{Y}_{..p}^{(SR_1...R_KD)} = \mathbf{H}^{(R_KD)} D_p(\mathbf{G}_K) \left[\prod_{i=2}^{K} \mathbf{H}^{(R_{i-1}R_i)} D_p(\mathbf{G}_{i-1}) \right] \mathbf{H}^{(SR_1)} D_p(\mathbf{G}_0) \mathbf{S}^T \in \mathbb{C}^{M_D \times N}, \quad (3.22)$$

and $\mathbf{V}_{..p}^{(SR_1R_2D)}$ is the global noise that contains all the noises in the channels with its gains.

Equation (3.21) corresponds to a PARATUCK-(K+1) decomposition [15] that can be rewritten in scalar form as

$$y_{m_D,n,p}^{(SR_1...R_KD)} = \sum_{m_{R_K}=1}^{M_{R_K}} ... \sum_{m_{R_1}=1}^{M_{R_1}} \sum_{m_S=1}^{M_S} h_{m_D,m_{R_K}}^{(R_KD)} g_{p,m_{R_K}}^{(K)} h_{m_{R_K},m_{R_{K-1}}}^{(R_{K-1}R_K)} g_{p,m_{R_{K-1}}}^{(K-1)} ... h_{m_{R_1},m_S}^{(SR_1)} g_{p,m_S}^{(0)} s_{n,m_S}. \quad (3.23)$$

3.3 Proposed Receiver Algorithms

This subsection presents two new non-iterative algorithms in MIMO AF relay-assisted systems based on the Kronecker product. The first algorithm is called Least-Squares Kronecker Factorization (LS-KF), and it is based on factorizations of the Kronecker product matrix. The second algorithm is called Least-Squares Kronecker Rearrangement-Based (LS-KR), and it is based on a rearrangement of the Kronecker product matrix, in order to achieve a rank-1 matrix. In order to have a better presentation of the proposed algorithms, from now on, we will ignore the noise component in (3.20).

Before presenting the proposed algorithms, we will develop some mathematical expressions from the received signal matrix (3.21). In the next developments, the two following properties are used:

$$vec(\mathbf{ABC}^T) = (\mathbf{C} \otimes \mathbf{A}) vec(\mathbf{B}). \quad (3.24)$$

$$D_p(\mathbf{A}) \otimes D_p(\mathbf{B}) = D_p((\mathbf{A}^T \diamond \mathbf{B}^T)^T). \quad (3.25)$$

Applying Property (3.24) in (3.21) twice, we have:

$$vec(\mathbf{Y}_{..p}^{(SR_1...R_KD)}) = vec(\mathbf{H}^{(R_KD)} D_p(\mathbf{G}_K) \mathbf{H}^{(R_{K-1}R_K)} D_p(\mathbf{G}_{K-1}) ... \mathbf{H}^{(SR_1)} D_p(\mathbf{G}_0) \mathbf{S}^T) \in \mathbb{C}^{M_D N \times 1}, \quad (3.26)$$

$$\mathbf{y}_p^{(SR_1...R_KD)} = (\mathbf{S} \otimes \mathbf{H}^{(R_KD)}) vec(D_p(\mathbf{G}_K) \mathbf{H}^{(R_{K-1}R_K)} ... \mathbf{H}^{(SR_1)} D_p(\mathbf{G}_0)), \quad (3.27)$$

and

$$\mathbf{y}_p^{(SR_1...R_KD)} = (\mathbf{S} \otimes \mathbf{H}^{(R_KD)})(D_p(\mathbf{G}_0) \otimes D_p(\mathbf{G}_K))vec(\mathbf{H}^{(R_{K-1}R_K)}D_p(\mathbf{G}_{K-1})...D_p(\mathbf{G}_1)\mathbf{H}^{(SR_1)}). \tag{3.28}$$

Now applying (3.25) in (3.28), we get:

$$\mathbf{y}_p^{(SR_1...R_KD)} = (\mathbf{S} \otimes \mathbf{H}^{(R_KD)})D_p((\mathbf{G}_0^T \diamond \mathbf{G}_K^T)^T)vec(\mathbf{H}^{(R_{K-1}R_K)}D_p(\mathbf{G}_{K-1})...D_p(\mathbf{G}_1)\mathbf{H}^{(SR_1)}). \tag{3.29}$$

Let us define $\mathbf{G}_{0K} = (\mathbf{G}_0^T \diamond \mathbf{G}_K^T) \in \mathbb{C}^{M_{R_K}M_S \times P}$. Note that $\mathbf{G}_{0K}$ depends on the coding matrices of the first and last hops, i.e, the coding matrices of the source and of the last relay. (3.29) can be rewritten as:

$$\mathbf{y}_p^{(SR_1...R_KD)} = (\mathbf{S} \otimes \mathbf{H}^{(R_KD)})D_p(\mathbf{G}_{0K}^T)vec(\mathbf{H}^{(R_{K-1}R_K)}D_p(\mathbf{G}_{K-1})...D_p(\mathbf{G}_1)\mathbf{H}^{(SR_1)}), \tag{3.30}$$

$$\mathbf{y}_p^{(SR_1...R_KD)} = (\mathbf{S} \otimes \mathbf{H}^{(R_KD)})diag(vec(\mathbf{H}^{(R_{K-1}R_K)}D_p(\mathbf{G}_{K-1})...D_p(\mathbf{G}_1)\mathbf{H}^{(SR_1)}))(\mathbf{G}_{0K}^T)_{p.}^T, \tag{3.31}$$

and

$$\mathbf{y}_p^{(SR_1...R_KD)} = (\mathbf{S} \otimes \mathbf{H}^{(R_KD)})diag(vec(\mathbf{H}_{..p}^{(G)}))(\mathbf{G}_{0K})_{.p} \in \mathbb{C}^{M_DN \times 1}. \tag{3.32}$$

with

$$\mathbf{H}_{..p}^{(G)} = \mathbf{H}^{(R_{K-1}R_K)}D_p(\mathbf{G}_{K-1})...D_p(\mathbf{G}_1)\mathbf{H}^{(SR_1)} \in \mathbb{C}^{M_{R_K} \times M_S}. \tag{3.33}$$

where $\mathbf{H}_{..p}^{(G)}$ is the matrix that contains all the channels and its gains. Assuming that the matrices $\mathbf{G}_1$, ..., $\mathbf{G}_{K-1}$ have equal rows (making them independents of p) and stacking the vectors $\mathbf{y}_p^{(SR_1...R_KD)}$ for $p = 1, ..., P$ into a matrix, we have:

$$\mathbf{Y}_1^{(SR_1...R_KD)} = \left[\mathbf{y}_1^{(SR_1...R_KD)} \dots \mathbf{y}_P^{(SR_1...R_KD)}\right] = (\mathbf{S} \otimes \mathbf{H}^{(R_KD)})D(vec(\mathbf{H}^{(G)}))\mathbf{G}_{0K} \in \mathbb{C}^{M_DN \times P}, \tag{3.34}$$

where $\mathbf{H}^{(G)} = \mathbf{H}_{..p}^{(G)}$, for $p = 1, ..., P$. That leads to

$$\mathbf{Y}_1^{(SR_1...R_KD)} = (\mathbf{S} \otimes \mathbf{H}^{(R_KD)})diag(\mathbf{h}^{(G)})\mathbf{G}_{0K} \in \mathbb{C}^{M_DN \times P}, \tag{3.35}$$

where $\mathbf{h}^{(G)}$ is the vectorized form of $\mathbf{H}^{(G)}$. Assume that $\mathbf{G}_{0K}$ has a right inverse, i.e. $\mathbf{G}_{0K}\mathbf{G}_{0K}^{\dagger} = \mathbf{I}_{M_{R_K}M_S}$. This means that the rank of $\mathbf{G}_{0K}$ is equal to $M_{R_K}M_S$, which implies $P \geq M_{R_K}M_S$, From

(3.35), we may then write:

$$\mathbf{Y}_1^{(SR_1...R_KD)}\mathbf{G}_{0K}^{\dagger} = (\mathbf{S} \otimes \mathbf{H}^{(R_KD)})diag(\mathbf{h}^{(G)}) \in \mathbb{C}^{M_DN \times M_{R_K}M_S}. \tag{3.36}$$

3.3.1 *Least-Squares Kronecker Factorization (LS-KF) Algorithm*

Let us define $\mathbf{W}$ as

$$\mathbf{W} = (\mathbf{S} \otimes \mathbf{H}^{(R_KD)})diag(\mathbf{h}^{(G)}) \in \mathbb{C}^{M_DN \times M_{R_K}M_S}. \tag{3.37}$$

The first step of the LS-KF algorithm consists in estimating $\mathbf{W}$ from (3.37) by means of the Least Squares (LS) method. Then, we estimate $\mathbf{S}$ and $\mathbf{H}^{(R_KD)}$ using several SVDs of the columns of $\mathbf{W}^{est}$, where $\mathbf{W}^{est}$ is the LS estimation of $\mathbf{W}$. This procedure, denoted Kronecker Factorization (KF), is based on the fact that $unvec(\mathbf{W}_{.j}) = \mathbf{H}_{.m_r}^{(R_KD)}\mathbf{S}_{.i}^T h_j^{(G)}$, with $j = (i-1)M_{R_K} + m_r$, is a rank-1 matrix, which means that $\mathbf{S}_{.i}$ and $\mathbf{h}_{.m_r}^{(R_KD)}$, with $i = 1, ..., M_S$, $m_r = 1, ..., M_{R_K}$, are optimally estimated as the first right- and left-singular vectors of $unvec(\mathbf{W}_{.j}^{est})$, respectively. The estimation of the columns of these matrices will have scalar ambiguities, that is

$$\mathbf{H}_{.m_r}^{(R_KD)^{est}} = \mathbf{H}_{.m_r}^{(R_KD)}\alpha_{m_r}, \tag{3.38}$$

and

$$\mathbf{S}_{.i}^{est} = \mathbf{S}_{.i}\alpha_i. \tag{3.39}$$

where α_{m_r} and α_i are scalars. The ambiguities are related, such that

$$\alpha_{m_r}\alpha_i = h_j^{(G)}. \tag{3.40}$$

α_i can be estimated assuming that the first row of $\mathbf{S}$ is known (this can be done using a few pilot symbols), so we have

$$\alpha_i = \frac{\mathbf{S}_{i1}^{est}}{\mathbf{S}_{i1}}. \tag{3.41}$$

At the end, we will have M_S estimations of $\mathbf{S}$ and M_{R_K} estimations of $\mathbf{H}^{(R_KD)}$ with scalar ambiguities in each column of these matrices. We take the first of these estimations. We cannot estimate these matrices without ambiguities, they are inherent to the model. However, as above mentioned, we can eliminate the ambiguities of $\mathbf{S}$ assuming that we know its first row, this is possible by using one pilot symbol by transmission stream. In the $\mathbf{H}^{(R_KD)}$ case, we cannot eliminate its ambiguity, but, we assume that we know its first row just to plot the simulation results.

The global channel matrix $\mathbf{H}^{(G)}$ (i.e $unvec(\mathbf{h}^{(G)})$) is estimated, using the first row of $\mathbf{W}^{est}$ and assuming the knowledge of $s_{1,i}$, that is

$$h_j^{(G)^{est}} = \frac{w_{1,j}^{est}}{s_{1,i} h_{m_r}^{(R_K D)^{(est)}}}. \tag{3.42}$$

with $i = 1, ..., M_S$, $m_r = 1, ..., M_{R_K}$ and

$$j = (i-1)M_{R_K} + m_r. \tag{3.43}$$

Note that $h_j^{(G)^{est}}$ will also have a scalar ambiguity. Indeed, as $h_{m_r}^{(R_K D)^{(est)}}$ has a scalar ambiguity, given in (3.38), it is easy to see that $h_j^{(G)^{est}}$ will have the following ambiguity:

$$h_j^{(G)^{est}} = \frac{h_j^{(G)}}{\alpha_{m_r}}, \tag{3.44}$$

which leads to

$$\mathbf{h}^{(G)^{est}} = \frac{\mathbf{h}^{(G)}}{\alpha_{m_r}}. \tag{3.45}$$

Such ambiguities cannot be eliminated, once we do not have knowledge of α_{m_r}. The LS-KF algorithm is summarized in Algorithm 1, where $\mathbf{S}_1^{est}$ and $\mathbf{H}_1^{(R_K D)^{est}}$ denote, respectively, the estimations of $\mathbf{S}$ and $\mathbf{H}^{(R_K D)}$ obtained by the first time during the Kronecker factorization.

Algorithm 1 - (LS-KF)

$\mathbf{W}^{est} \leftarrow \tilde{\mathbf{Y}}_1^{(SR_1 ... R_K D)} \mathbf{G}_{0K}^{\dagger}$;
for $j = 1$ to $M_{R_K} M_S$ **do**
  $\mathbf{Z}_{.j} \leftarrow unvec(\mathbf{W}_{.j}^{est})$;
  $\mathbf{U}\mathbf{\Sigma}\mathbf{V}^H \leftarrow SVD(\mathbf{Z}_{.j})$;
  $\mathbf{S}_{.j}^{est} \leftarrow \mathbf{V}_{.1}^{*}$;
  $\mathbf{H}_{.j}^{(R_K D)^{est}} \leftarrow \mathbf{U}_{.1}$;
end for
for $i = 1$ to M_S **do**
  for $m_r = 1$ to M_{R_K} **do**
    $j \leftarrow (i-1)M_{R_K} + m_r$;
    $h_j^{(G)^{est}} \leftarrow \frac{w_{1,j}^{est}}{s_{1,i} h_{m_r}^{(R_K D)^{est}}}$;
  end for
end for
$\mathbf{S}^{est} \leftarrow \mathbf{S}_1^{est}$;
$\mathbf{H}^{(R_K D)^{est}} \leftarrow \mathbf{H}_1^{(R_K D)^{est}}$;

3.3.2 *Least-Squares Kronecker Rearrangement-Based (LS-KR) Algorithm*

In [16], it is proposed a rearrangement in a given Kronecker product matrix in order to achieve a rank-1 matrix. Given a matrix $\tilde{\mathbf{W}} = \mathbf{S} \otimes \mathbf{H}^{(R_K D)} \in \mathbb{C}^{M_D N \times M_{R_K} M_S}$, where $\mathbf{S} \in \mathbb{C}^{N \times M_S}$ and $\mathbf{H}^{(R_K D)} \in \mathbb{C}^{M_D \times M_{R_K}}$, we can express $\tilde{\mathbf{W}}$ as

$$\tilde{\mathbf{W}} = \begin{bmatrix} \tilde{\mathbf{W}}_{11} & \tilde{\mathbf{W}}_{12} & \dots & \tilde{\mathbf{W}}_{1M_S} \\ \tilde{\mathbf{W}}_{21} & \tilde{\mathbf{W}}_{22} & \dots & \tilde{\mathbf{W}}_{2M_S} \\ \vdots & \vdots & \ddots & \vdots \\ \tilde{\mathbf{W}}_{N1} & \tilde{\mathbf{W}}_{N2} & \dots & \tilde{\mathbf{W}}_{NM_S} \end{bmatrix}, \tag{3.46}$$

where $\tilde{\mathbf{W}}_{ij} \in \mathbb{C}^{M_D \times M_{R_K}}$. The rearrangement $\mathcal{R}(\tilde{\mathbf{W}})$ of the matrix $\tilde{\mathbf{W}}$ is given by

$$\mathcal{R}(\tilde{\mathbf{W}}) = \begin{bmatrix} \tilde{\mathbf{W}}_1 \\ \tilde{\mathbf{W}}_2 \\ \vdots \\ \tilde{\mathbf{W}}_{M_S} \end{bmatrix}, \tag{3.47}$$

$$\tilde{\mathbf{W}}_j = \begin{bmatrix} vec(\tilde{\mathbf{W}}_{1j})^T \\ vec(\tilde{\mathbf{W}}_{2j})^T \\ \vdots \\ vec(\tilde{\mathbf{W}}_{Nj})^T \end{bmatrix}, j = 1, ..., M_S. \tag{3.48}$$

We note that $\mathcal{R}(\tilde{\mathbf{W}}) \in \mathbb{C}^{NM_S \times M_D M_{R_K}}$ and is given by

$$\mathcal{R}(\tilde{\mathbf{W}}) = vec(\mathbf{S}) vec(\mathbf{H}^{(R_K D)})^T. \tag{3.49}$$

However, our matrix $\mathbf{W}$ is not only the Kronecker product of the matrices $\mathbf{S}$ and $\mathbf{H}^{(R_K D)}$. This way, we cannot ensure that $\mathcal{R}(\mathbf{W})$ is a rank-1 matrix, so we will use $\mathbf{W}_m$ to estimate the parameters.

The first step of this algorithm is the same as the previous one, that is, estimate $\mathbf{W}$ in (3.37), by a least-squares technique. Once we cannot assure that $\mathcal{R}(\mathbf{W})$ is a rank-1 matrix, due to the presence of the diagonal matrix containing the elements of the global channel in (3.37), we cannot estimate the matrices $\mathbf{S}$ and $\mathbf{H}^{(R_K D)}$ with a single SVD (optimal case), so we will estimate them with several

SVDs using $\mathbf{W}_m$ defined as

$$\mathbf{W}_m = \begin{bmatrix} vec(\mathbf{W}_{1m})^T \\ \vdots \\ vec(\mathbf{W}_{Nm})^T \end{bmatrix} \in \mathbb{C}^{N \times M_D M_{R_K}}, \tag{3.50}$$

where $\mathbf{W}_{nm}$ is the nm^{th} sub-block of $\mathbf{W} \in \mathbb{C}^{M_D N \times M_{R_K} M_S}$ (or n^{th} row of $\mathbf{W}_m$) given by

$$\mathbf{W}_{nm} = \mathbf{H}^{(R_K D)} s_{nm} diag(\mathbf{h}_m^{(G)}). \tag{3.51}$$

Thus,

$$vec(\mathbf{W}_{nm})^T = s_{nm} vec(\mathbf{H}^{(R_K D)})^T diag(\mathbf{1}_{M_D \times 1} \otimes \mathbf{h}_m^{(G)}). \tag{3.52}$$

Another form of $\mathbf{W}_m$ can be written as

$$\mathbf{W}_m = \mathbf{S}_{.m} vec((\mathbf{H}^{(R_K D)})^T) diag(\mathbf{1}_{M_D \times 1} \otimes \mathbf{h}_m^{(G)}). \tag{3.53}$$

This procedure, denoted by Kronecker Rearrangement (KR), is based on the fact that $\mathbf{W}_m$ is a rank-1 matrix, which means that $\mathbf{S}_{.m}$ and $vec(\mathbf{H}^{(R_K D)})^T$, with $m = 1, ..., M_S$, are optimally estimated as the first left- and right-singular vectors of $\mathbf{W}_{.m}^{est}$, respectively. In order to estimate $\mathbf{H}^{(R_K D)}$ we need to use the $unvec(\cdot)$ operator in $vec(\mathbf{H}^{(R_K D)})^T$.

At the end, there will be M_S estimations of $\mathbf{H}^{(R_K D)}$ and one estimation of $\mathbf{S}$. So, for the $\mathbf{H}^{(R_K D)}$ we take the first of these estimations.

From (3.53), it can be viewed that the estimated parameters have the same ambiguities as in (3.38)-(3.40). Moreover, the ambiguities of $\mathbf{S}$ can be eliminated assuming that its first row is known (this can be done using a few pilot symbols) and using (3.41). In the $\mathbf{H}^{(R_K D)}$ estimation, its ambiguities cannot be eliminated, since we do not have the knowledge of $h_j^{(G)}$. But, we eliminate it by assuming that we know the first row of $\mathbf{H}^{(R_K D)}$ just to plot the simulation results.

The LS-KR algorithm is summarized in Algorithm 2. The global channel is estimated in the same way as in the previous algorithm, i.e, using (3.42).

3.3.3 *Identifiability Conditions*

Once the proposed algorithms are non-iterative, we do not need to worry about the uniqueness conditions. Regarding the identifiability issues, choosing the matrices $\mathbf{G}_i$, with $i = 1, ..., K-1$, with equal rows, and $\mathbf{G}_K$ and $\mathbf{G}_0$ matrices such that $\mathbf{G}_{0K}$ has a right inverse, will ensure that the algorithms will provide identifiable estimations of the symbols and channels matrices. $P \geq M_{R_K} M_S$ is then a

Algorithm 2 - (LS-KR)

$\mathbf{W}^{est} \leftarrow \tilde{\mathbf{Y}}_1^{(SR_1 \ldots R_K D)} \mathbf{G}_{0K}^{\dagger}$;
for $m = 1$ to M_S **do**
  $\mathbf{W}_m^{est} \leftarrow \begin{bmatrix} vec(\mathbf{W}_{1m}^{est})^T \\ \vdots \\ vec(\mathbf{W}_{Nm}^{est})^T \end{bmatrix}$;
  $\mathbf{U}\mathbf{\Sigma}\mathbf{V}^H \leftarrow SVD(\mathbf{W}_m)$;
  $\mathbf{S}_{.m}^{est} \leftarrow \mathbf{U}_{.1}$;
  $\mathbf{H}^{(R_K D)^{est}} \leftarrow unvec(\mathbf{V}_{.1}^*)$;
end for
for $i = 1$ to M_S **do**
  for $m_r = 1$ to M_{R_K} **do**
    $j \leftarrow (i-1)M_{R_K} + m_r$;
    $h_j^{(G)^{est}} \leftarrow \frac{w_{1,j}^{est}}{s_{1,i} h_{m_r}^{(R_K D)^{est}}}$;
  end for
end for
$\mathbf{H}^{(R_K D)^{est}} \leftarrow \mathbf{H}_1^{(R_K D)^{est}}$;

necessary condition.

Chapter 4

SIMULATION RESULTS

In this chapter, simulation results aiming to evaluate the performance of the proposed receivers by means of Monte Carlo samples are presented. The metrics of performance used are the SER and the channels NMSE, given by

$$\text{NMSE} = \frac{1}{S_{MC}} \left(\sum_{s=1}^{S_{MC}} \frac{||\mathbf{H}_s - \hat{\mathbf{H}}_s||_F^2}{||\mathbf{H}_s||_F^2} \right), \tag{4.1}$$

where S_{MC} is the number of Monte Carlo samples, and $\mathbf{H}_s$ and $\hat{\mathbf{H}}_s$ represents the channel matrix and the estimated channel matrix at the s^{th} run, respectively. $\mathbf{H}$ can be either the $\mathbf{H}^{(R_K D)}$ or the $\mathbf{H}^{(G)}$ channel.

For all the simulations, it was considered the parameters shown in Table 4.1, when not stated otherwise. Also, all the channels are assumed to have Rayleigh flat fading and the elements of the channel matrices are i.i.d.

The total transmission power was equally divided between the source and the relay nodes. Also, the relays were placed in a uniform way through the source-destination path. The code matrices were randomly generated with gaussian distribution, and the elements of all the coding matrices are i.i.d.

The proposed receivers were compared to the iterative receiver called PARATUCK2-ALS, proposed in [9]. This receiver uses only the relay-assisted link (no direct source-destination available) and is based on the ALS algorithm. Also, the proposed receivers were compared to the PARATUCK2 Zero Forcing (PARATUCK2-ZF), that estimates the **S** matrix assuming that all the channels are known (the optimal case), that is

$$\mathbf{S}_{ZF}^{est} = \mathbf{H}_{eff}^{\dagger} \tilde{\mathbf{Y}}_2, \tag{4.2}$$

where $\tilde{\mathbf{Y}}_2$ is the noisy mode-2 unfolded matrix of the tensor $\mathcal{Y}$, that represents the received signal by the destination through the relay assisted link, and $\mathbf{H}_{eff}$ is the effective channel given by all the

Table 4.1: Parameters used in the computational simulations.

Monte Carlo runs	10^4
Number of symbols (N)	100
Number of relays (K)	2
QAM modulation order	16
Path-loss coeficient	4
Number of transmission blocks (P)	8
Total transmission power	1
Source-destination distance	1
Number of antennas at the source (M_S)	2
Number of antennas at the relay k (M_{R_k})	2
Number of antennas at the destination (M_D)	2

channels and coding matrices, i.e

$$\mathbf{H}_{eff} = \mathbf{H}^{(R_K D)} D_p(\mathbf{G}_K) \mathbf{H}^{(R_{K-1} R_K)} D_p(\mathbf{G}_{K-1}) ... \mathbf{H}^{(SR_1)} D_p(\mathbf{G}_0). \tag{4.3}$$

4.1 SER Analysis

Figure 4.1 shows how the SER behaves as the SNR increases varying the number of relays for the two proposed receivers. We can see that the LS-KR receiver always provides a better SER if comparing to the LS-KF receiver. This is due to the following reason. When we estimate **S** via SVD of a rank-1 matrix, we are eliminating the noise subspace. The optimal case would be to estimate the parameters using a SVD of the matrix **W**. However, this is not possible. Nevertheless, as the LS-KF uses $M_{R_K} M_S$ SVDs, and the LS-KR uses only M_S SVDs, we can see that the LS-KR one uses less SVDs, being more close to the optimal case, providing, this way, a better performance. Also, we can see in Figure 4.1 that, as the number of relays increases, the receivers provide a smaller SER. This is expected, because, once we use more relays, we will have shorter distances between the nodes, needing less transmission power to communicate due to the less severe path-losses.

Figure 4.2 shows how the SER behaves as the SNR increases for a fixed number of relays ($K = 2$) and varying the number of antennas at the destination, for the two proposed receivers. We can see that as the number of antennas at the destination increases, the receivers provide a smaller SER. This is a benefit of the additional spatial diversity provided by the antenna array at the destination. Also, the LS-KR always provides a smaller SER if comparing to the LS-KF, due to the reason explained before.

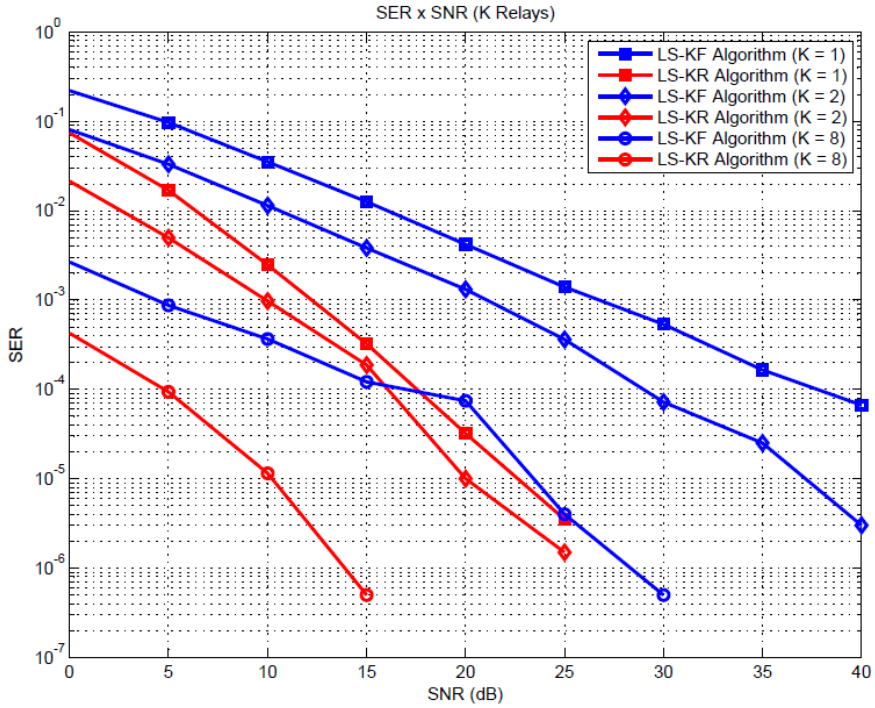

Fig. 4.1: SER *versus* SNR varying the number of relays.

In Figure 4.3 we can see how the SER behaves as the SNR increases varying the number of transmission blocks, for the two proposed receivers. We can see that the performance of both algorithms is improved as P increases, this is due to the coding gain provided by the number of transmission blocks.

In Figure 4.4 we can see how the SER behaves as the SNR increases, comparing the proposed receivers to the PARATUCK2-ALS proposed in [9] and the PARATUCK2-ZF receivers. In this simulation it was considered a single relay ($K = 1$) and $M_D = M_S = M_{R_k} = 2$. Also, it was used a 4-QAM modulation and 8 transmission blocks ($P = 8$). For the PARATUCK2-ALS receiver, the threshold for convergence was set to 10^{-6}. We can see that both algorithms have a better performance if comparing to the PARATUCK2-ALS for low SNRs, since they are non-iterative, being estimated via SVD, with no convergence problems. We can see, also, that the LS-KR SER curve is approximately 5dB way from the PARATUCK2-ZF SER curve, the optimal case.

4.2 NMSE Analysis

It is shown in Figure 4.5 how the NMSE of the channel $\mathbf{H}^{(R_K D)}$ behaves as the SNR increases varying the number of relays, for the two proposed receivers. As in the previous figure, we can see

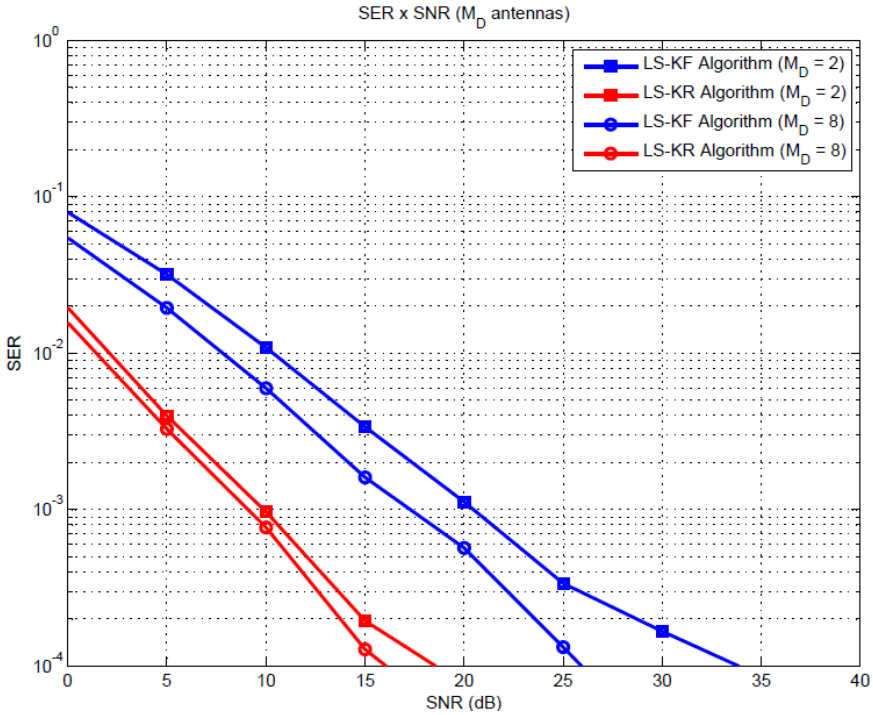

Fig. 4.2: SER *versus* SNR varying the number of antennas at the destination.

that the performance is better when the number of relays increases, also due to the reason previous explained, that is, due to the less severe path-loss. We can see either that the LS-KR receiver always provides a better estimation of the channel if comparing to the LS-KF receiver, due to the same reason of Figure 4.1.

Figure 4.6 illustrates how the NMSE of the $\mathbf{H}^{(R_K D)}$ channel behaves as the SNR increases, using the same parameters of Figure 4.3 and varying P. The same improvement in Figure 4.3 we can see here in Figure 4.6, in the estimation of the channel $\mathbf{H}^{(R_K D)}$, due to the reason explained in Figure 4.3.

We can see in Figure 4.7 how the NMSE of the channel $\mathbf{H}^{(R_K D)}$ behaves as the SNR increases for the LS-KF, LS-KR and the PARATUCK2-ALS receivers. In this simulation, the same parameters as in Figure 4.4 were used. We can see that the both proposed receivers provide a better estimation, if comparing to the PARATUCK2-ALS receiver, due to the reason explained in the previous subsection.

Figure 4.8 shows how the NMSE of the global channel $\mathbf{H}^{(G)}$ behaves as the SNR increases by varying the number of relays, for the two proposed receivers. We can see that the performance is practically the same as for the LS-KF and LS-KR algorithms for the same number of relays, once $\mathbf{H}^{(G)}$ is estimated in the same way for both algorithms. As expected, the performance is better when the number of relays increases, due to the reason previously explained.

Figure 4.9 illustrates how the NMSE of the global channel $\mathbf{H}^{(G)}$ behaves as the SNR increases, using the same parameters of Figures 4.3 and 4.6 and varying P. The same improvement showed in

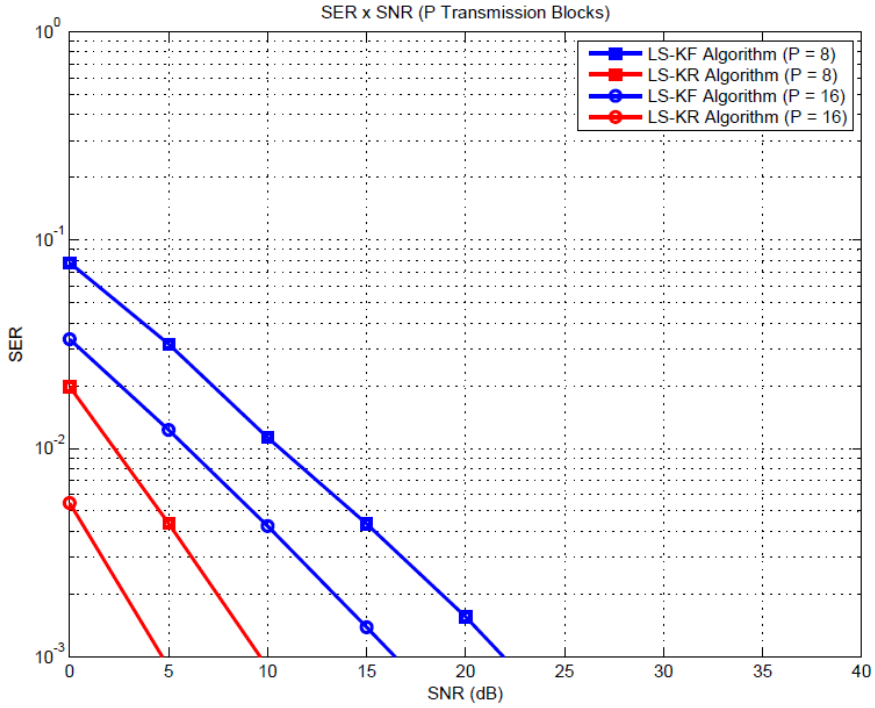

Fig. 4.3: SER *versus* SNR varying the number of transmission blocks.

those figures is also showed here in Figure 4.9. The reason is the same as explained in Figure 4.3.

Figure 4.10 shows a comparison between the estimation of the channels $\mathbf{H}^{(R_K D)}$ and $\mathbf{H}^{(G)}$. We can see that the channel $\mathbf{H}^{(R_K D)}$ is better estimated than the global channel $\mathbf{H}^{(G)}$. This is expected, since we cannot estimate $\mathbf{H}^{(G)}$ with a SVD, we estimate it with an equation that contains the noisy matrix $\mathbf{W}^{est}$, estimated by the LS method. Regarding $\mathbf{H}^{(R_K D)}$, we can estimate it using SVDs, eliminating the noise subspace.

In Figure 4.11 we can see how the NMSE of the channel $\mathbf{H}^{(SR_1)}$ behaves as the SNR increases for the LS-KF, LS-KR and the PARATUCK2-ALS receivers. Note that, from the definition of $\mathbf{H}^{(G)}$ in (3.33), when $K = 1$, we have $\mathbf{H}^{(G)} = \mathbf{H}^{(SR_1)}$. The same parameters as in Figures 4.4 and 4.7 were used in this simulation. We can see that all the receivers provide practically the same performance. The PARATUCK2-ALS is iterative, estimating $\mathbf{H}^{(SR_1)}$ from random initialization, so its performance depends on this initialization. The LS-KF and the LS-KR estimates $\mathbf{H}^{(SR_1)}$ using the noisy matrix $\mathbf{W}^{est}$, the LS estimation of the matrix $\mathbf{W}$.

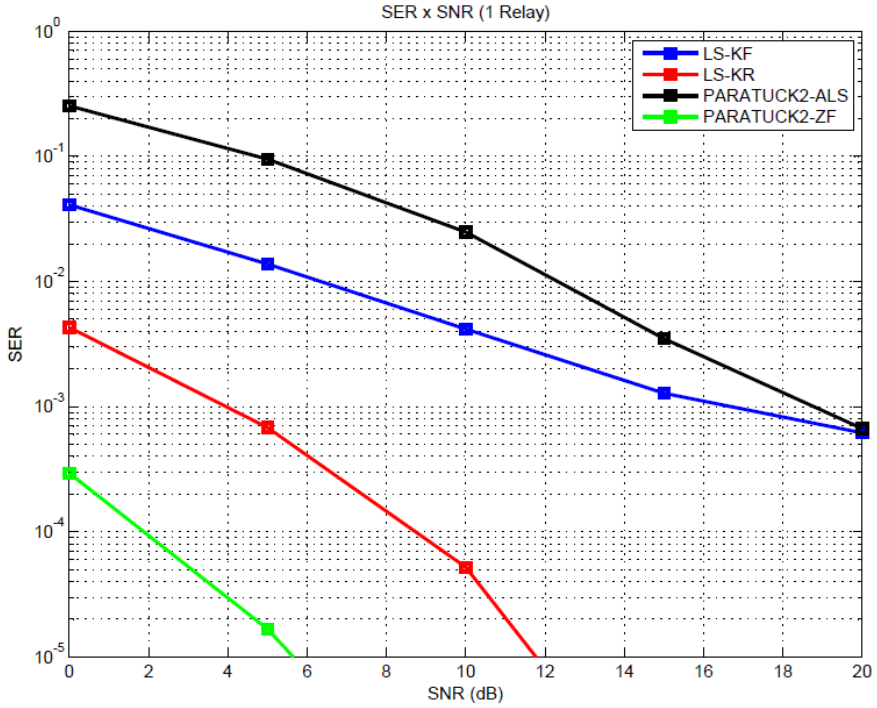

Fig. 4.4: SER *versus* SNR for the LS-KF, LS-KR, PARATUCK2-ZF and PARATUCK2-ALS receivers.

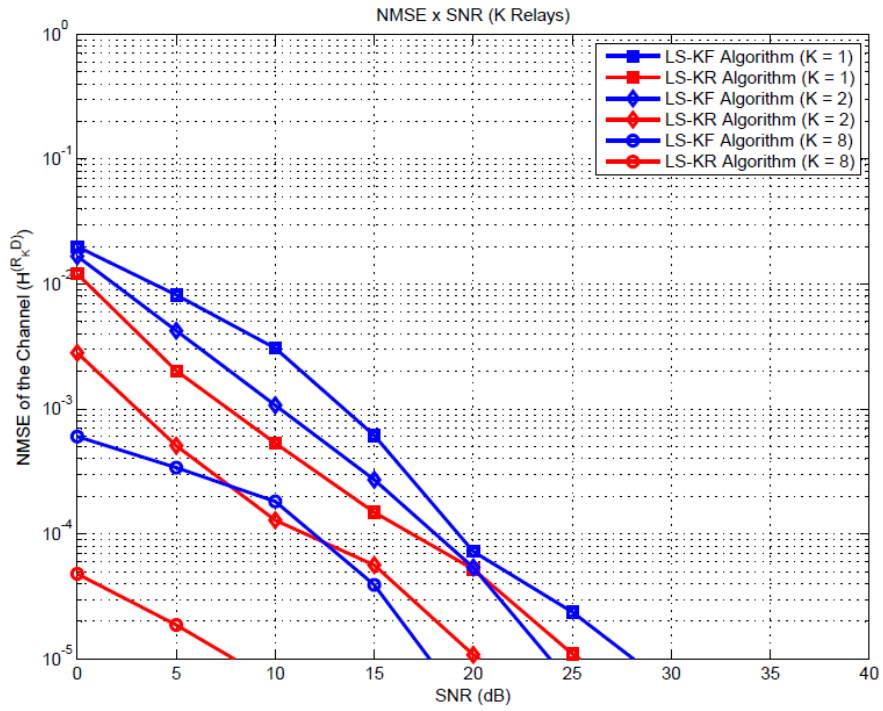

Fig. 4.5: NMSE of $\mathbf{H}^{(R_K D)}$ *versus* SNR varying the number of relays.

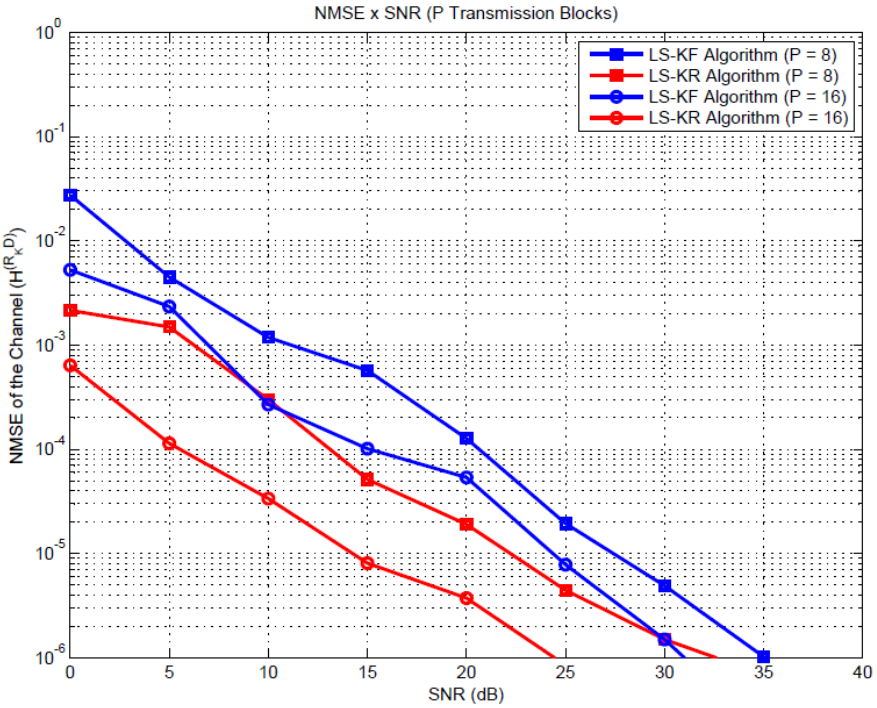

Fig. 4.6: NMSE of $\mathbf{H}^{(R_K D)}$ *versus* SNR varying the number of transmission blocks.

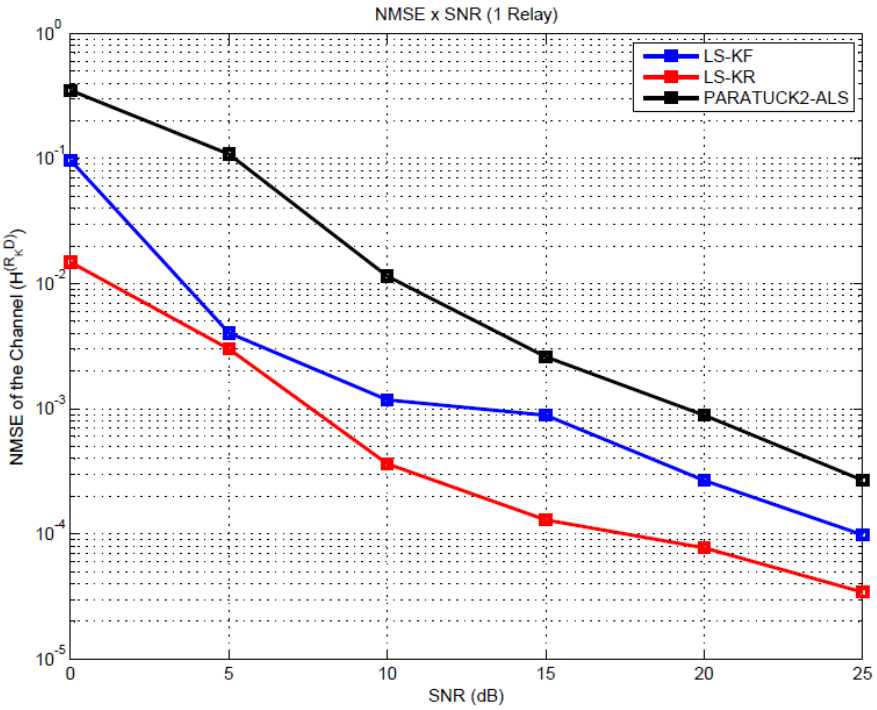

Fig. 4.7: NMSE of $\mathbf{H}^{(R_1 D)}$ *versus* SNR for the LS-KF, LS-KR and PARATUCK2-ALS receivers.

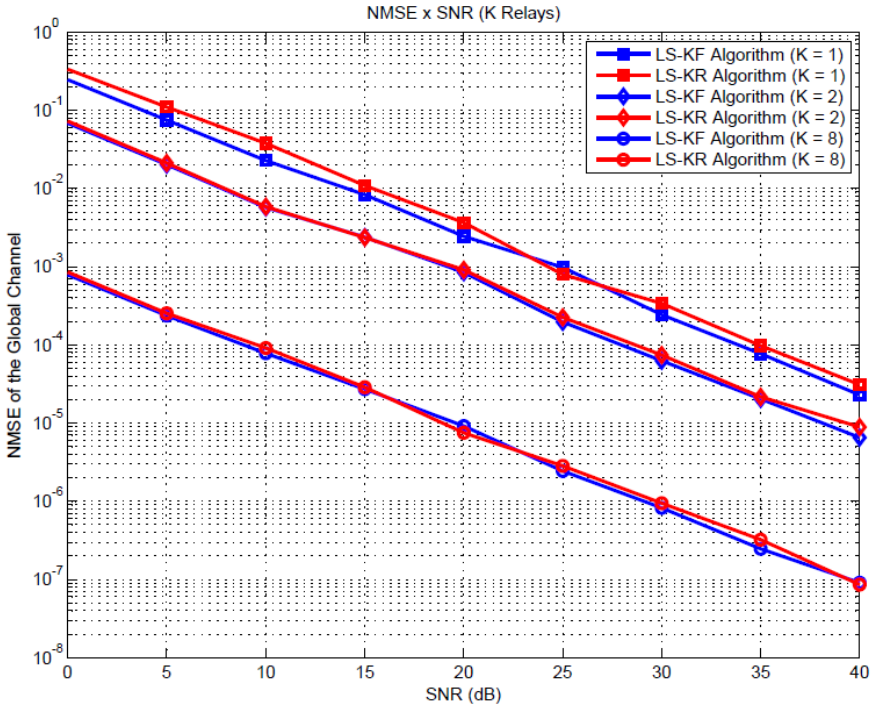

Fig. 4.8: NMSE of $\mathbf{H}^{(G)}$ *versus* SNR varying the number of relays.

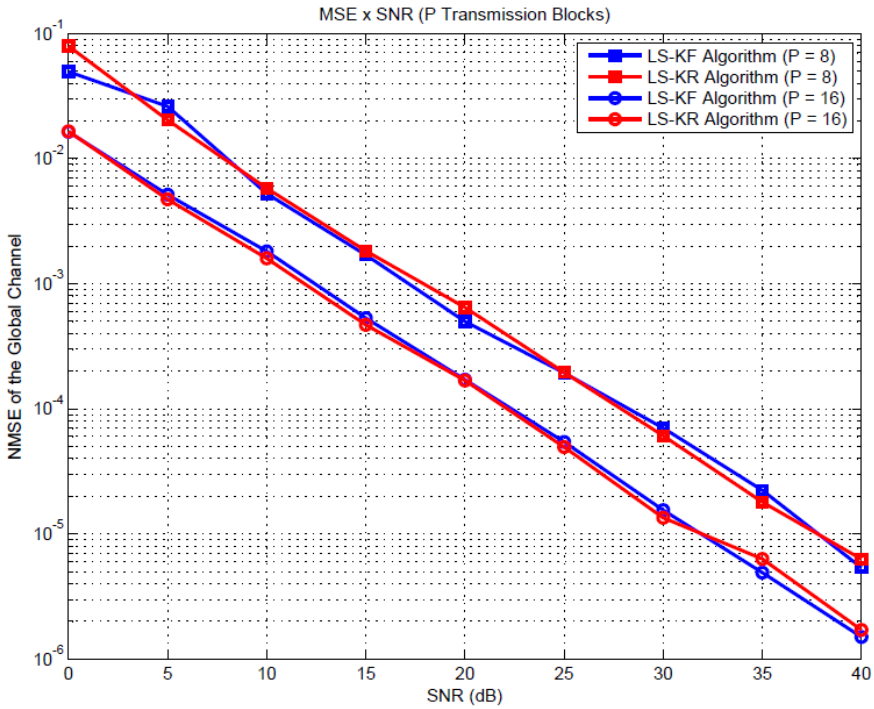

Fig. 4.9: NMSE of $\mathbf{H}^{(G)}$ *versus* SNR varying the number of transmission blocks.

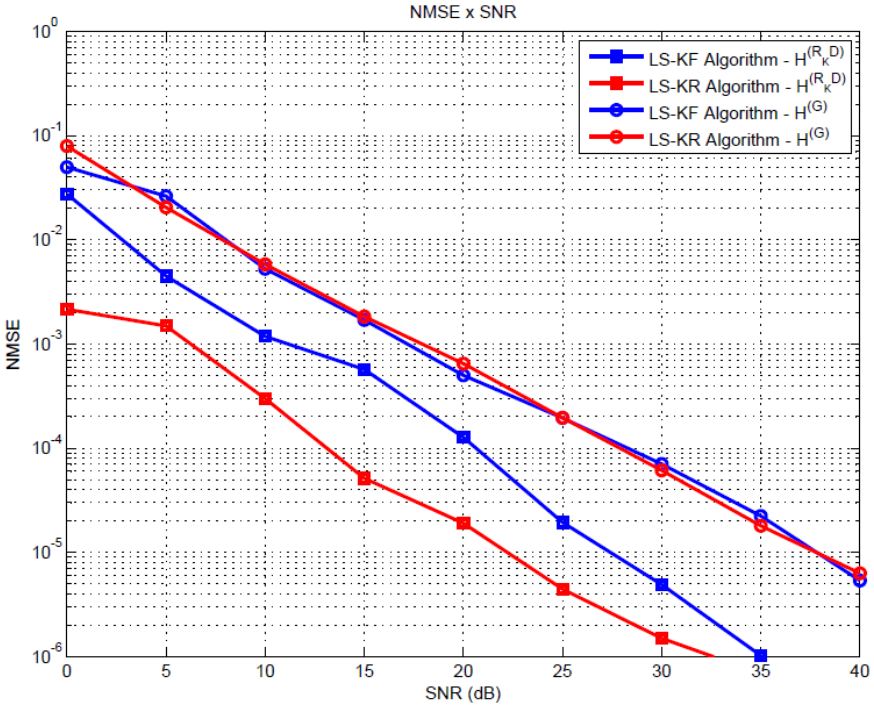

Fig. 4.10: NMSE of $\mathbf{H}^{(R_K D)}$ and $\mathbf{H}^{(G)}$ *versus* SNR.

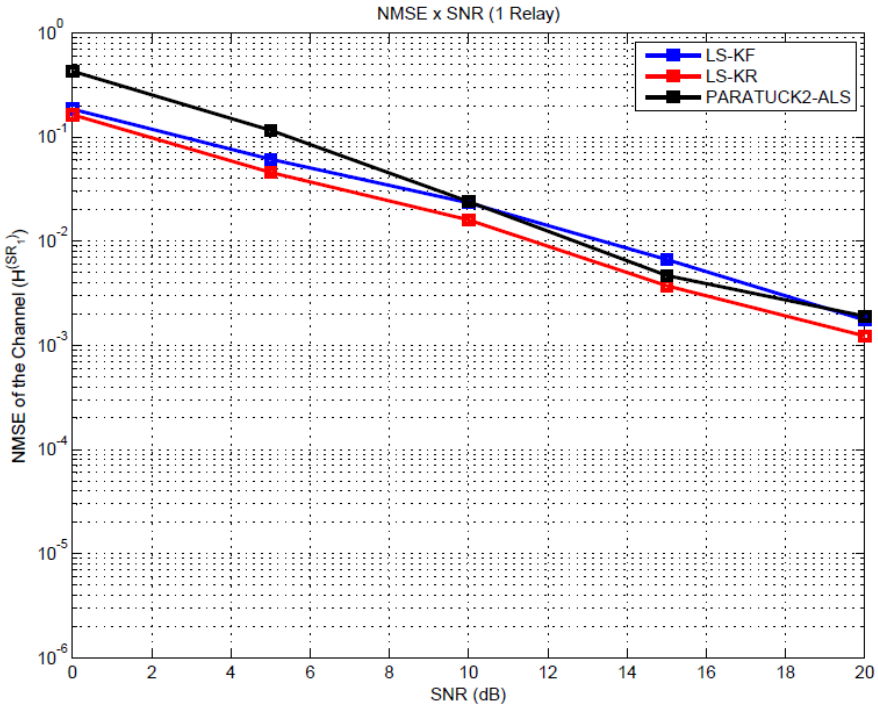

Fig. 4.11: NMSE of $\mathbf{H}^{(SR_1)}$ *versus* SNR for the LS-KF, LS-KR and PARATUCK2-ALS receivers.

Chapter 5

CONCLUSIONS AND PERSPECTIVES

The present work has as major contributions the proposition of two new semi blind receivers that jointly estimate the symbols and channels matrices in a multi-hop MIMO relay-assisted system, using a KRST coding at the source combined with the AF protocol at the relays. The proposed receivers were derived from the modeling of the received signals as a PARATUCK-N tensor decomposition. One of the algorithms, called LS-KF, is based on a factorization of the Kronecker product, while the other, called LS-KR, is based on a rearrangement of this Kronecker product in order to achieve a rank-1 matrices. It was shown that both algorithms are efficient in semi-blind estimating both the symbols and the channel matrices, providing a low SER as well as a low NMSE. Also, it was shown that the identifiability conditions of these algorithms are easy to achieve and that there is no uniqueness issues.

Each algorithm has shown to have a better performance regarding the SER and the estimation of the channels $\mathbf{H}^{(R_K D)}$ and $\mathbf{H}^{(G)}$ with the increasing of the number of relays, the antennas at the destination and transmission blocks. Comparing the quality of these two channel estimations, we saw that $\mathbf{H}^{(R_K D)}$ is better estimated, since it can be estimated via SVD (which cancels out the noise subspace), while the global channel $\mathbf{H}^{(G)}$ cannot be estimated using the SVD, being estimated using an equation with the LS estimation of the $\mathbf{W}$ matrix.

We saw that the performance of the multi-hop case is better than the two-hop case, due to the less severe path-loss, needing less transmission power by the nodes to transmit the data signal, as explained before. Regarding the two-hop scenario, the proposed receivers were compared with an ALS-based receiver proposed in [9] and the PARATUCK2-ZF. The proposed receivers showed to have a better performance than the iterative algorithm proposed in [9], specially for low SNRs, and very close to PARATUCK2-ZF, specially the LS-KR.

Also, we saw in the simulation results that the LS-KR algorithm has a better performance when compared with the LS-KF technique, regarding the SER and the estimation of the $\mathbf{H}^{(R_K D)}$ channel.

This happens because we are eliminating the noise subspace when we estimate $\mathbf{S}$ via SVD. Indeed, the LS-KR is closer to the optimal case (to estimate using a single SVD), once the LS-KR one uses less SVDs, than the LS-KF. Regarding the estimation of the global channel $\mathbf{H}^{(G)}$, we saw that both algorithms have practically the same performance, since both of them use the same equation to estimate this parameter.

In future works, we plan to generalize these semi-blind receivers to other scenarios, as OFDM systems, CDMA systems, etc. Also, we aim aim to develop other estimation algorithms. Specifically, the objectives of future works are:

- Generalize the proposed semi-blind receivers to other scenarios, as OFDM and CDMA systems, and using multiples relays in a parallel way, for example.
- Develop other estimation algorithms, based on the ALS, for example.
- Use another coding structures at the source, as, for example, the TST coding.
- Analysis of the performance and comparison with other receivers in the literature.

REFERENCES

[1] LIU, K. J. R.; SADEK, A. K.; SU, W.; KWASINSKI, A. **Cooperative Communications and Networking**. Cambridge University Press, 2009.

[2] PLEVEL, S.; TOMAZIC, S.; JAVORNIK, T.; KANDUS, G. **MIMO:** Wireless Communications, Encyclopedia of Wireless and Mobile Communications, DOI: 10.1081/E-EWMC-120043484. 2008.

[3] SIDIROPOULOS, N. D.; BRO, R.; GIANNAKIS, G. B. Parallel Factor Analysis in Sensor Array Processing, **IEEE Transactions on Signal Processing**, v. 48, n. 8, p. 2377-2388, Aug. 2000.

[4] SIDIROPOULOS, N. D.; GIANNAKIS, G. B.; BRO, R. Blind PARAFAC Receivers for DS-CDMA Systems, **IEEE Transactions on Signal Processing**, v. 48, n. 3, p. 810-823, Mar. 2000.

[5] ALMEIDA, A.; FAVIER, G. Double Khatri-Rao Space-Time-Frequency Coding Using Semi-Blind PARAFAC Based Receiver, **IEEE Signal Processing Letters**, May, 2013.

[6] ALMEIDA, A.; FAVIER, G.; MOTA, J.C.M. PARAFAC-Based Unified Tensor Modeling of Wireless Communication Systems with Application to Blind Multiuser Equalization, **Signal Processing - Special Issue on Tensor Signal Processing**, v. 87, n. 2, p. 337-351, Feb. 2007.

[7] FERNANDES, C.; ALMEIDA, A.; COSTA, D. United Tensor Modeling for Blind Receivers in Multiuser Uplink Cooperative Systems, **IEEE Signal Processing Letters**, v. 19, n. 5, p. 247-250, 2012.

[8] ALMEIDA, A.; FERNANDES, C.; COSTA, D. Multiuser Detection for Uplink DS-CDMA Amplify-and-Forward Relaying Systems, **IEEE Signal Processing Letters**, v. 20, n. 7, p. 697-700, Jul. 2013.

[9] XIMENES, L.; ALMEIDA, A.; FAVIER, G. PARAFAC-PARATUCK Semi-Blind Receivers for Two-Hop Cooperative MIMO Relay Systems, **IEEE Transactions on Signal Processing**, v. 62, n. 14, July 15, 2014.

[10] XIMENES, L.; FAVIER, G.; ALEMIDA, A. Semi-Blind Receivers for Non-Regenerative Cooperative MIMO Communications Based on Nested PARAFAC Modeling, **IEEE Transactions on Signal Processing**, Sep. 2015.

[11] FAVIER, G.; FERNANDES, C.; ALMEIDA, A. Nested Tucker Tensor Decomposition with Application to MIMO Relay Systems Using Tensor Space-time Coding (TSTC), **Signal Processing**, n. 128, p. 318-331, Nov. 2016.

[12] COSTA, M.; FAVIER, G.; ALMEIDA, A.; ROMANO, J. Tensor Space-Time (TST) Coding for MIMO Wireless Communication Systems, **Signal Processing**, v. 92, n. 4, p. 1079-1092, 2012.

[13] ALMEIDA, A.; FAVIER G.; XIMENES, L. Space-time-frequency (STF) MIMO communication systems with blind receiver based on a generalized PARATUCK2 model, **IEEE Transactions on Signal Processing**, Apr, 2013.

[14] SIDIROPOULOS, N.D.; BUDAMPATI, R.S. Khatri-Rao space-time codes, **IEEE Transactions on Signal Processing**, v. 50, n. 10, p. 2396-2407, Oct. 2002.

[15] HARSHMAN, R.A.; LUNDY, M.E. Uniqueness Proof for a Family of Models Sharing Features of Tucker's Three-Mode Factor Analysis and PARAFAC/CANDECOMP, **Psychometrika**, v. 61, n. 1, p. 133-154, Mar. 1996.

[16] VAN LOAN, C.; PITSIANIS, N. **Approximation with Kronecker Products**, Linear Algebra for Large Scale and Real-Time Applications, p. 293-314. Cornell University. 1993.

[17] KOLDA, T.G.; BADER, B.W. Tensor Decompositions and Applications. **SIAM J. Matrix Anal. Appl.** 51(3), p. 455-500, Jun 2008.

[18] COMON, P. **Tensor Decompositions:** State of the Art and Applications. In IMA Conf. Mathematics in Signal Process., Warwick, UK, Dec. 18-20 2000.

[19] DE LATHAUWER, L. **Signal Processing Based on Multilinear Algebra**. PhD thesis, Katholieke Univ. Leuven, Leuven, Belgium, 1997.

[20] http://www.cs.nthu.edu.tw/∼jungchuk/image/cooperative.jpg <Accessed in 25/05/2017 at 12:58 pm>

[21] HE, X. **Cooperative Communications in Wireless Local Area Networks:** MAC Protocol Design and Multi-layer Solutions. A Dissertation Submitted in Partial Fulfillment of the Requirements for the Degree of *Philosophiae Doctor*(PhD) in Mobile Communication Systems: Network, Security and Formal Methods. University of Agder. 2012.

[22] GOLDSMITH, A. **Wireless Communications**. Cambridge University Press. Stanford University, 2005.

[23] ALMEIDA, A.; FAVIER, G.; MOTA, J.C.M. Space-time spreading-multiplexing for MIMO wireless communication systems using the PARATUCK-2 tensor model. **Elsevier Signal Processing**, p. 2103-2116, 2009.

[24] ALMEIDA, A. **Tensor Modeling and Signal Processing for Wireless Communication Systems**. PhD thesis, Université de Nice-Sophia Antipolis, Nice, France, 2007.

[25] TUCKER, L.R. Some mathematical notes on three-mode factor analysis. **Psychometrika**, 31:279-311, 1966.

[26] HARSHMAN, R.A. Foundations of the PARAFAC procedure: Model and conditions for an "explanatory" multi-mode factor analysis. UCLA **Working Papers in Phonetics**, 16:1-84, Dec. 1970.

[27] CARROLL, J.D.; CHANG, J. Analysis of individual differences in multidimensional scaling via an N-way generalization of "Eckart-Young" decomposition. **Psychometrika**, 35(3):283-319, 1970.

[28] HESKETH, T.J. **Detection and Resource Allocation Algorithms for Cooperative MIMO Relay Systems**. PhD thesis, University of York, Feb. 2014.

[29] FAVIER, G.; ALMEIDA, A. Tensor space-time-frequency coding with semi blind receivers for MIMO wireless communication systems, **IEEE Trans. Signal Process.**, v. 62, n. 22, p. 5987-6002, Nov. 2014.

[30] KREIMER, N.; SACCHI, M.D. **Rank Reduction of Unfolded Tensors for Pre-stack Denoising and Reconstruction**, CSEG RECORDER, Department of Physics, University of Alberta, Edmonton, Canada, 2012.

[31] KRUSKAL, J.B. Three-way arrays: Rank and uniqueness or trilinear decompositions, with applications to arithmetic complexity and statistics. **Linear Algebra Appl.**, 18:95-138, 1977.

[32] SOYSA, M.; SURAWEERA, H.A.; TELLAMBURA, C.; GARG, H.K. **Amplify-and-Forward Partial Relay Selection with Feedback Delay**. Wireless Communications and Networking Conference, March, 2011.

[33] ZHENG, L.; TSE, D. Diversity and Multiplexing: a Fundamental Tradeoff in Multiple Antenna Channels. **IEEE Trans. Inf. Theory.** 49(5), p. 1073-1096. 2003.

[34] OSELEDETS, I.V. Tensor-train decomposition, **SIAM J. Sci. Comput.** 33(5), p. 2295-2317. 2011.

[35] OSELEDETS, I.V.; TYRTYSHNIKOV, E. TT-cross approximation for multidimensional arrays, **Linear Algebra Appl.** 432, p. 70-88. 2010.